



HAL
open science

Concentrates from citrus juice obtained by crossflow microfiltration: Guidance of the process considering carotenoid bioaccessibility

Sophie Di Corcia, Claudie Dhuique-Mayer, Manuel Dornier

► To cite this version:

Sophie Di Corcia, Claudie Dhuique-Mayer, Manuel Dornier. Concentrates from citrus juice obtained by crossflow microfiltration: Guidance of the process considering carotenoid bioaccessibility. *Innovative Food Science & Emerging Technologies / Innovative Food Science and Emerging Technologies*, 2020, 66, pp.102526 -. 10.1016/j.ifset.2020.102526 . hal-03492696

HAL Id: hal-03492696

<https://hal.science/hal-03492696>

Submitted on 24 Oct 2022

HAL is a multi-disciplinary open access archive for the deposit and dissemination of scientific research documents, whether they are published or not. The documents may come from teaching and research institutions in France or abroad, or from public or private research centers.

L'archive ouverte pluridisciplinaire **HAL**, est destinée au dépôt et à la diffusion de documents scientifiques de niveau recherche, publiés ou non, émanant des établissements d'enseignement et de recherche français ou étrangers, des laboratoires publics ou privés.



Distributed under a Creative Commons Attribution - NonCommercial 4.0 International License

1 **Concentrates from citrus juice obtained by crossflow microfiltration: guidance**
2 **of the process considering carotenoid bioaccessibility**

3

4 Sophie di Corcia¹, Claudie Dhuique-Mayer^{1,2}, Manuel Dornier^{1*}

5

6 ¹ QualiSud, Univ Montpellier, Cirad, Institut Agro, Univ Avignon, Univ La Réunion, Montpellier, France

7 ² Cirad, UMR QualiSud, F-34398 Montpellier, France

8 *Corresponding author: manuel.dornier@supagro.fr

9

10 **ABSTRACT**

11 This work focused on an eco-friendly process to concentrate carotenoids from a citrus juice
12 formulated with clementine and pink grapefruit. It is based on crossflow microfiltration associated
13 with enzymatic liquefaction, diafiltration and pasteurization. The aim was to evaluate the impact of
14 the main operating conditions on the process performance and on the nutritional quality of the final
15 concentrate taking into account the bioaccessibility of β -carotene, β -cryptoxanthin and lycopene.
16 First, the best enzyme/pressure/membrane combination was chosen in order to maximize permeate
17 flux during microfiltration ($> 100 \text{ kg}\cdot\text{h}^{-1}\cdot\text{m}^{-2}$ at 2.6 bar with tubular inorganic membranes). Second
18 thanks to a Plackett-Burman experimental design applied to the whole process, we showed the
19 enzymatic dose was the most impacting parameter on carotenoid bioaccessibility and it decreased it.
20 An optimal dose of enzyme had to be defined in order to obtain a good compromise between the
21 process performance and the nutritional quality of the citrus concentrate.

22 **Keywords:** clementine/grapefruit based-product, carotenoid bioaccessibility, membrane process
23 performance.

24

25 **Nomenclature**

26 β_i : bioaccessibility of the carotenoid i (%)

27 $\partial J_p / \partial MRR$: coefficient of permeate flux instability ($\text{kg} \cdot \text{h}^{-1} \cdot \text{m}^{-2}$)

28 BC: β -carotene

29 BCX: β -cryptoxanthin

30 CMF: crossflow microfiltration

31 $D[4,3]$: particle diameter of which the volume corresponds to the average volume of all particles
32 (μm)

33 D_{10} : diameter below which 10% vol. of the particles are found (μm)

34 D_{50} : median diameter below which 50% vol. of the particles are found (μm)

35 D_{90} : diameter below which 90% vol. of the particles are found (μm)

36 DMR: diamass ratio (mass of distilled water added during the diafiltration stage divided by mass of
37 retentate)

38 J_p : permeate flux ($\text{kg} \cdot \text{h}^{-1} \cdot \text{m}^{-2}$)

39 LYC: lycopene

40 M_{liq} : liquefaction mode (batch or continuous)

41 MRR: mass reduction ratio

42 σ_{pore} : average pore diameter of the membrane (μm)

43 P_0 : pasteurization value (min)

44 RAE: retinol activity equivalent ($\mu\text{g}/250\text{g}$)

45 RAE*: retinol activity equivalent taking into account carotenoid bioaccessibility ($\mu\text{g}/250\text{g}$)

46 RDA: recommended dietary allowances (%)

47 SIS: suspended insoluble solids ($\text{g} \cdot \text{kg}^{-1}$)

48 Span: indicator of the width of the size distribution of the particle diameters (Equation 1)

49 TA: titratable acidity ($\text{g} \cdot \text{kg}^{-1}$)

50 T_{CMF} : temperature of crossflow microfiltration ($^{\circ}\text{C}$)

- 51 TDM: total dry matter (g.kg^{-1})
- 52 t_{liq} : enzymatic liquefaction time (min)
- 53 T_{liq} : temperature of enzyme liquefaction ($^{\circ}\text{C}$)
- 54 TmP: transmembrane pressure (bar)
- 55 TSS: total soluble solids (g.kg^{-1})
- 56 U: crossflow velocity (m.s^{-1})

57 **1. Introduction**

58 Citrus are the most cultivated fruits in the world and many varieties are produced (orange,
59 grapefruit, mandarins, tangerines, lemons and limes). A large amount of citrus fruits is consumed
60 worldwide in juice form. The consumption of citrus juices has grown rapidly since the '80s, from a
61 consumption of 3 to 22 L per year and inhabitant in Europe today (AIJN - Market Report 2017).
62 Moreover, 75% of citrus fruit production in Brazil, the top producing country in the world, is
63 processed into juice (USDA - World Markets and Trade 2020). Consumers perceive citrus juices,
64 especially orange juice, as a natural source of vitamin C and minerals, but they are also rich in a large
65 variety of phytochemicals such as carotenoids. Carotenoids are liposoluble pigments synthesized
66 mainly by plants and stored in the chromoplasts of plant cells in a solid-crystalline state or in a liquid-
67 crystalline form and/or a lipid-dissolved form (R. M. Schweiggert, Mezger, Schimpf, Steingass, &
68 Carle, 2012). Chromoplast morphology also varies (globular, crystalline, membranous, fibrillary and
69 tubular) depending on the fruit, and between different tissues of the same fruit (R. Schweiggert &
70 Carle, 2017; Zhang et al., 2019). In addition to giving an attractive color to citrus juice, carotenoids
71 have many health benefits: antioxidant, antidiabetic, anti-inflammatory and anti-cancer (Bungau et
72 al., 2019; Lee, Hu, Park, & Lee, 2019; Sun, Tao, Huang, Ye, & Sun, 2019). Several studies have also
73 shown that the consumption of carotenoid-rich food is linked to a reduced risk of developing certain
74 chronic diseases such as cardiovascular disease, cataracts or cancer (Lee et al., 2019; Rodriguez-
75 Concepcion et al., 2018; Carla M Stinco et al., 2019). However, the most relevant role is the pro-
76 vitamin A activity attributed to carotenoids containing at least one unsubstituted β -ionone ring such
77 as α -carotene, β -carotene and β -cryptoxanthin and can be converted into vitamin A by the specific
78 enzyme β -carotene oxygenase. Vitamin A plays a key function in vision, embryonic development,
79 reproduction and cellular growth and differentiation (Kopec & Failla 2018). Although carotenoids are
80 present in significant amounts in citrus juices, their health effects are limited by their bioavailability
81 including their bioaccessibility. Carotenoid bioaccessibility, which is one of the main factors
82 governing bioavailability, corresponds to the proportion of carotenoids released from the food

83 matrix and transferred into mixed micelles that can be then absorbed by the human intestinal cells
84 (Poulaert, Borel, Caporiccio, Gunata, & Dhuique-Mayer, 2012). Therefore, carotenoids must be
85 released from the chromoplasts in order to reach the lipid phase and be incorporated into the mixed
86 micelles and be available for intestinal absorption. In fact, bioavailability depends on several factors
87 among which food matrix and its technological processing are the more important. Some studies
88 have shown that the release of carotenoids from their food matrix was strongly influenced by the
89 physical shape of the chromoplasts (R. Schweiggert & Carle, 2017; R. M. Schweiggert et al., 2012;
90 Zhang et al., 2019). Better liberation and bioaccessibility of carotenoids from non-crystalline
91 chromoplasts was reported by Schweiggert, Mezger et al. 2012. On the other hand, mechanical and
92 thermal treatments applied to foods can modify their nutritional quality and increase carotenoid
93 bioaccessibility (Barba, Saraiva, Cravotto, & Lorenzo, 2019; Cilla et al., 2012; Knockaert, Lemmens,
94 Van Buggenhout, Hendrickx, & Van Loey, 2012; Kopec & Failla, 2018). These treatments destroyed
95 cell structure, from the cell wall to the membrane of organelles such as chromoplast membranes
96 promoting carotenoid release. Thermal treatments, widely used in food industry for stabilization and
97 preservation, conduce to cell disorganization mainly through depolymerization and solubilization of
98 pectic polysaccharides (Lemmens, Van Buggenhout, Oey, Van Loey, & Hendrickx, 2009) that has led
99 to better understand the effects on carotenoid bioaccessibility. Other studies showed that cooking
100 and grinding can increase lycopene bioaccessibility (J. Aschoff et al., 2015; J. K. Aschoff et al., 2015;
101 Carla M. Stinco et al., 2012; Carla M Stinco et al., 2019). The impact of the process has also been
102 studied on citrus juices: the carotenoid bioaccessibility in pasteurized juices is higher than in fresh
103 juices (J. K. Aschoff et al., 2015; Carla M. Stinco et al., 2012). Moreover, for humans, the
104 bioavailability of β -carotene and β -cryptoxanthin is higher for pasteurized orange juice than for fresh
105 juice (J. Aschoff et al., 2015).

106 Crossflow microfiltration (CMF), an eco-friendly membrane process, allows the clarification and
107 stabilization of fruit juices (Dornier, Belleville, & Vaillant, 2018; Maktouf et al., 2014; Mierczynska-
108 Vasilev & Smith, 2015) as well as the concentration of hydrophobic compounds without heating

109 (Chaparro et al., 2016; de Abreu et al., 2013; Polidori, Dhuique-Mayer, & Dornier, 2018). Indeed,
110 hydrophobic compounds, which are associated with insoluble solids, are generally retained by the
111 membrane. Thus, it is possible to increase carotenoid content in retentate up to 10 fold by using this
112 physical separation process to obtain a carotenoid-rich concentrate without heating or using organic
113 solvent.

114 However, this process results in a concentrate with physical characteristics that are considerably
115 different from those of juice and so could affect carotenoid bioaccessibility. In addition, viscosity and
116 pectin content increase with increasing carotenoid content during CMF. L. Gence, Servent,
117 Poucheret, Hiol, and Dhuique-Mayer (2018) have already compared the effect of CMF on the
118 carotenoid bioaccessibility between concentrates made with fresh and pasteurized juices and they
119 showed that bioaccessibility was strongly correlated to the pectin content and structure. The aim of
120 this study was to go further and to focus on a more complete process including the CMF step and
121 several other unit operations (enzymatic liquefaction, diafiltration and pasteurization). Within this
122 context, the work expected to evaluate the impact of the main operating conditions on process
123 performance and on nutritional quality of the final concentrate through carotenoid bioaccessibility in
124 order to optimize the process. This one, including various steps, was originally guided by carotenoid
125 bioaccessibility for the production of citrus concentrates. Another main goal was to understand how
126 different processing steps could affect carotenoid bioaccessibility.

127

128

129 **2. Materials and methods**

130

131 **2.1. Materials**

132 Flash-pasteurized clementine (*Citrus clementina* Hort. ex Tan.) and pink grapefruit (*Citrus paradisi*
133 Macf.) juices were purchased in a local supermarket (Saint-Clément de Rivière, France). Packaged in
134 aseptic carton packs, these industrial 100% pure juices, i.e. without any additives in accordance with
135 current regulations, were stored at 4 °C for two weeks before processing (no significant change in
136 carotenoid profile highlighted during storage). A formulation obtained from 60/40 (v/v) *C. clementina*
137 / *C. paradisi* juices was chosen in order to obtain a product containing at a time the 3 carotenoids β -
138 cryptoxanthin, β -carotene and lycopene each with an interesting concentration on a nutritional point
139 of view. Three different lots of juice were purchased with volumes ranging from 10 kg to 50 kg.

140

141 **2.2. Processing**

142 All the unit operations constituting the process are detailed in **Figure 1**. Citrus juices underwent
143 several operations, the main one being crossflow microfiltration (CMF). First, an enzymatic pre-
144 liquefaction of the juices was carried out in order to decrease viscosity and limit membrane fouling
145 during CMF. Widely used in the juice industry, this step guarantees good performance of the process
146 (F. Vaillant et al., 1999). After concentration of carotenoids by microfiltration, a diafiltration step
147 allowed the purification of the carotenoids by removing soluble solids, mainly sugars and organic
148 acids. A final pasteurization step was added to stabilize the product eliminating the microorganisms
149 retained in the concentrate.

150

151 **2.2.1. Enzymatic liquefaction**

152

153 Two commercial enzyme mixtures, Ultrazym AFP and Pectinex Ultra SP from Novozymes (Denmark),
154 commonly used for filtration and clarification of fruit juices (Sandri, Fontana et al. 2011, Bajpai 2012),
155 were compared. They consist of a mixture of enzymes (mainly pectinases associated with secondary
156 activities such as hemicellulases) that allow the hydrolysis of the structural polysaccharides of cell
157 walls especially pectic compounds. Activity spectra of these two mixtures are different with
158 pectinesterase as preponderant activity for Pectinex and polygalacturonase for Ultrazym (Macedo,
159 Robrigues, Pinto, & de Brito, 2015). Citrus concentrates were treated with enzymes ($50 - 300 \mu\text{L kg}^{-1}$)
160 either prior to microfiltration (batch) or during microfiltration (continuous) (M_{liq}), at a temperature
161 T_{liq} of 30 or 50°C. In the batch mode, all the juice was treated with enzyme prior to microfiltration for
162 45-90 min while in the continuous mode the system was continuously fed by juice and enzyme (for
163 every 100 g of permeate discharged, feeding by 100 g of juice with enzyme).

164

165 **2.2.2. Concentration by crossflow microfiltration and purification by diafiltration**

166 The crossflow microfiltration device (TIA, Bollène, France), described by Polidori et al. (2018), was
167 constituted of a 3 L feed tank, connected to 4 housings each containing a single-tubular ceramic
168 membrane mounted in series (**Table 1**). The crossflow circulation of the suspension was ensured by a
169 positive displacement pump with an eccentric rotor (model PCM, Moineau, Levallois-Perret, France).
170 The temperature of the juice in the pilot unit (T_{CMF}) was regulated by a jacketed heat exchanger
171 connected to a cryostat (model F34, Julabo GmbH, Seelbach, Germany). The transmembrane
172 pressure (T_{mP}), controlled by a backpressure valve, was measured using manometers located at the
173 inlet and the outlet of the circulation loop. The crossflow velocity (U) in the loop could vary from 2 to
174 $5 \text{ m}\cdot\text{s}^{-1}$ thanks to a frequency converter connected to the pump. Depending on the purpose of the
175 filtration test, the trial could be conducted at a constant mass reduction ratio MRR of 1 (total
176 recycling of permeate and retentate, i.e, without concentration) or increasing MRR (removing
177 permeate and compensating with raw juice in the feed, i.e., with concentration). In that case, the

178 permeate flux J_p was monitored as a function of MRR. In order to facilitate comparisons between the
179 trials, the average permeate flux between MRR 3 and 4.4 was chosen. A permeate flux instability
180 coefficient $\partial J_p / \partial \text{MRR}$ was defined as the slope of J_p as a function of MRR. The lower the coefficient,
181 the more stable the permeate flux.

182 A diafiltration step can follow concentration in order to purify retentate using distilled water as a
183 solvent. After concentration up to MMR 4.4, diafiltration was conducted with a constant volume
184 compensating the mass of extracted permeate by an equal mass of distilled water added to the feed
185 tank. The diamass ratio (DMR) was defined as the ratio between the total mass of distilled water
186 added to the tank and the mass of circulating retentate. In our trials, diafiltration was stopped when
187 the DMR reached approximately 1.0.

188

189 **2.2.3. Pasteurization**

190 According to Gates (2012) and the standard practices in the industry, citrus concentrates were
191 pasteurized choosing a pasteurization value P_0 of 100 min as a target (reference temperature 70°C
192 and z-value 10°C). The concentrate was distributed in several 15 mL glass tubes and put in a water
193 bath at 80°C. Thanks to a thermal probe placed into one tube, the temperature of the concentrate
194 was measured every minute and the P_0 was calculated according to the standard Ball procedure.
195 When the targeted P_0 was reached (after 14 min), the tubes were quickly immersed in an ice-cold
196 water bath to cool down and stop the treatment.

197

198

199 **2.3. Analyses**

200

201 **2.3.1. Physico-chemical parameters**

202 *pH and titratable acidity*

203 The pH of citrus juices and concentrates and their titratable acidity were measured using a Titroline
204 titrator (Schott Schweiz AG, St. Gallen, Switzerland). The pH was measured with a pH probe,
205 previously calibrated with buffer solutions of pH 4 and 7. The titratable acidity was measured by
206 titration with 0.1 mol.L⁻¹ NaOH up to pH 8.3 and expressed as citric acid content per kg of juice or
207 concentrate.

208

209 *Soluble and insoluble fractions*

210 Juices and concentrates were analyzed for total soluble solids (TSS) using a refractometer at 25°C
211 (Pocket PAL-1, 0-53% Brix, ATAGO, Tokyo), total dry matter (TDM) (2.0 g of concentrate dried in an
212 oven at 70°C under vacuum at 100 mPa for 24 h) and suspended insoluble solids (SIS). For SIS, 5.0 g
213 of concentrate were weighed in previously weighed 15 mL falcon tubes. The samples were then
214 centrifuged at 1900 x g, for 20 min, at room temperature (centrifuge 5810 R, Eppendorf, Hamburg,
215 Germany). After centrifugation, the supernatant was removed in order to retain only the insoluble
216 particles in the pellet. Then, the pellet was washed twice in succession with water: it was re-
217 suspended in 10 mL of distilled water, vortexed and centrifuged for 20 min. The supernatant was
218 removed and the last pellet was dried in an oven at 70°C for about 24 h. The mass ratio between the
219 dry base and the initial quantity thus represents the SIS content.

220

221 *Rheological properties*

222 Flow rheological measurements were carried out on juices and concentrates with a Physica imposed
223 stress rheometer (model MCR301, Anton Paar GmbH, Graz, Austria), equipped with a duvet
224 geometry measurement module (double concentric cylinder, ref. DG27 / T2000 / SS) and
225 accompanied by Rheoplus software for data acquisition. The temperature was regulated at 25°C
226 using a Peltier effect system connected to a refrigerant (Viscotherm VT2, Anton Paar GmbH, Graz,
227 Austria). The limit apparent viscosity for a shear rate of 1000 s⁻¹ was chosen to compare
228 concentrates. Indeed, this value is close to that evaluated on the membrane surface in the CMF
229 system (Dahdouh et al., 2015).

230

231 *Particle size and distribution*

232 Measurements of juice particle size were made with a Laser diffraction granulometer (Mastersizer
233 3000, Malvern Instruments Limited, Worcestershire, UK). Values of 1.73 and 1.33 were used
234 respectively as refractive indices for particles and the liquid phase of the suspension, the particle
235 absorption index being 0.1. (Corredig, Kerr, & Wicker, 2001; Dahdouh, Delalonde, Ricci, Ruiz, &
236 Wisniewski, 2018). The samples were diluted, introduced into the feed tank with an obscuration value
237 of about 30% for juices and 15% for concentrates and then agitated at 1500 rpm. In these
238 experimental conditions, the particle size distribution was assumed not to be affected. For each
239 measurement, the particle size distribution was obtained in volume. The mean volume diameter
240 D[4,3], which indicates the particle diameter of which the volume corresponds to the average
241 volume of all the particles in the sample (called the DeBrouckere mean), was deducted from the
242 measured distribution. The span, that characterizes the width of the distribution of particle sizes in
243 the suspension was also calculated (Equation 1).

244

Equation 1

$$Span = \frac{D_{90} - D_{10}}{D_{50}}$$

245 with D_{50} the median diameter, D_{10} and D_{90} the diameters below which 10% and 90% of the particles
246 are found.

247

248 *Turbidity*

249 The turbidity was measured using a turbidimeter (model LP 2000, Hanna instruments, Szeged,
250 Hungary) which measures the intensity of the light (890 nm) scattered by the suspension, the angle
251 between the detector and the light source being 90°. Before each measurement, the turbidimeter
252 was calibrated using two standard formazin solutions at 0 and 10 NTU. Measurements were made on
253 concentrates diluted 30 folds in distilled water in order to respect the accuracy range of the
254 turbidimeter and results were expressed taking into account the dilution factor.

255

256 **2.3.2. Carotenoid analysis**

257

258 2.3.2.1. Carotenoid content

259 *Extraction*

260 Carotenoid extraction, carried out according to the method described by Gies, Descalzo, Servent, and
261 Dhuique-Mayer (2019), has been optimized and applied to citrus juices and concentrates. Two g of
262 juice or 0.5 g of concentrate mixed with 0.5 mL distilled water were homogenized in a glass tube (20
263 mL). Two mL ethanol with 1% pyrogallol were added and then the mixture was vortexed
264 (homogenized). The tube was then placed in a water-bath at 70°C for 2-3 min, protected from light.
265 Two mL of KOH 12 mol.L⁻¹ was added and the mixture was vortexed and set in a water bath at 70°C
266 for 30 min. After cooling in an ice bath, 2 mL of distilled water was added to help the phase shift. The
267 extraction was carried out twice with 5 mL of hexane. The hexane phase was pooled and evaporated
268 under nitrogen in a water bath at 37°C. The dry extracts were dissolved in 500 µL of CH₂Cl₂ and 500

269 μL of methyl tert-butyl ether (MTBE)/methanol mixture (4:1, v/v) in an amber vial before injection in
270 HPLC.

271 *HPLC analysis*

272 HPLC carotenoid analyses were performed according to a previous study (Poulaert et al. 2012) with
273 an Agilent 1100 system equipped with a diode array detector and autosampler. The column used was
274 a C30 YMC column (250 x 4.6 mm; 5 μm , YMC Europe GMBH, Germany). The flow rate was 1 $\text{mL}\cdot\text{min}^{-1}$,
275 the analysis temperature 25°C and the injection volume 20 μL . The mobile phases were water
276 (eluent A), methanol (eluent B) and MTBE (eluent C) that follow the gradient described by Gleize,
277 Steib, André, and Reboul (2012). The absorbance was measured at 450 nm to identify β -carotene
278 (BC), β -cryptoxanthin (BCX) and 470 nm for lycopene (LYC). Chromatographic data and UV-Visible
279 spectra (Agilent ChemStation Plus software) allowed the different carotenoids to be identified.
280 Quantification of carotenoids was achieved using external calibration curves with 5 concentration
281 levels from 2 to 15 $\text{mg}\cdot\text{L}^{-1}$ for the BC standard, from 10 to 40 $\text{mg}\cdot\text{L}^{-1}$ for BCX and from 7 to 50 $\text{mg}\cdot\text{L}^{-1}$
282 for LYC.

283

284 2.3.2.2. Carotenoid bioaccessibility

285

286 *In vitro digestion*

287 The *in vitro* digestion model used in our study was initially developed by Reboul et al. (2006)
288 especially for carotenoids. It had been validated against human studies and was considered to be a
289 reliable model for carotenoid behavior during *in vitro* digestion (Etcheverry, Grusak, & Fleige, 2012).
290 This model was adapted for citrus juices according to Dhuique-Mayer et al. (2007). Briefly, 30.0 g of
291 juice or 5.0 g of concentrate were mixed with 32 mL of a 0.9% NaCl solution. The mixture was
292 incubated in a stirring water bath at 37°C for 10 min, and protected from light. To simulate the
293 gastric digestion phase, the pH was adjusted to 4.0 with 1 $\text{mol}\cdot\text{L}^{-1}$ NaOH, then 2 mL of pepsin was
294 added before incubating the mixture at 37°C for 30 min. To simulate the duodenal phase, the pH of

295 the gastric mixture was raised to 6.0 by adding 20 mL of 0.45 mol.L⁻¹ sodium bicarbonate. Then, 9 mL
296 of a solution containing porcine pancreatin (2 mg.mL⁻¹) and porcine bile extract (12 mg.mL⁻¹) in 100
297 mmol.L⁻¹ trisodium citrate were added, as well as 4 mL for juice or 2 mL for concentrate of porcine
298 bile extract (0.1 g.mL⁻¹) and 1 mL of cholesterol esterase (10 mg at 32 Unit.mL⁻¹ in 6 mL of distilled
299 water). Samples were subsequently incubated in a shaking water bath at 37°C for 30 min to finish the
300 digestion process. Micelles were separated by centrifugation at 48 000 x g for 4 h at 10°C using an
301 Avanti JE rotor JA-20 (Beckman-coulter, USA), and the aqueous fraction was collected and filtered
302 through a 0.20 µm filter (Whatman, U.K.). Aliquots were stored at -20 °C until analysis.

303

304 *Carotenoids from Micellar phase analysis*

305 Carotenoid extraction from digested samples was performed as previously described by Dhuique-
306 Mayer et al. (2018). An aliquot of 10 mL of the micellar phase from a digested sample was extracted
307 3 times with 10 mL of hexane and 5 mL of ethanol containing 100 µL of β-apo-8'-carotenal (at 24.4
308 mg.L⁻¹) as an internal standard. The collected hexanic phases were dried with anhydrous sodium
309 sulphate. The pooled hexane extracts were evaporated and dissolved in 250 µL of CH₂Cl₂/250 µL of
310 the MTBE/methanol (4:1, v/v) before HPLC analysis according to the analytic conditions described
311 below for carotenoid analysis.

312 Bioaccessibility of a carotenoid i, noted β_i, was calculated according to Equation 2 and expressed in
313 percentage (%).

314 *Equation 2*

$$315 \beta_i = 100 \frac{m_i}{m_{i0}}$$

316 m_i: amount of carotenoid i in the micellar phase (mg)

317 m_{i0}: amount of carotenoid i in the initial sample of citrus juice or concentrate (mg)

318

319 2.3.3. Vitamin A activity equivalent calculation

320 Vitamin A activity equivalent was expressed in terms of retinol activity equivalents RAE (Equation 3).
321 The RAE value was widely used for food. Another vitamin A activity equivalent RAE*, taking into
322 account carotenoid bioaccessibility, was defined using Equation 4. Results were referred to 250 g of
323 product corresponding to an average glass of beverage. Moreover, the percentage of Recommended
324 Dietary Allowances (RDA) provided by 250 g of juice or concentrate could be deduced considering
325 that 800 µg of RAE is recommended for an adult (> 18 years old) per day (Medicine, 2001) (National
326 Institutes of Health, Office of Dietary Supplements, 2020).

327 *Equation 3*

$$RAE = \frac{[BC] \times 250}{12} + \frac{[BCX] \times 250}{24}$$

$$RAE^* = \frac{[BC] \times 250}{12} \times \frac{\beta_{BC}}{100} + \frac{[BCX] \times 250}{24} \times \frac{\beta_{BCX}}{100}$$

328 *Equation 4*

329

330 [BC]: β-carotene content (mg.kg⁻¹)

331 [BCX]: β-cryptoxanthine content (mg.kg⁻¹)

332 β_i: Bioaccessibility of carotenoid i (%)

333

334 2.4. Experimental approach

335 The chosen experimental strategy was organized in 3 successive phases:

336 - the first phase focused on the CMF operation. It aimed to choose the 3 main operating parameters,
337 i.e., membrane, transmembrane pressure (TmP) and enzyme mixture. It was based mainly on the
338 permeate flux without considering carotenoid bioaccessibility in order to reduce the screening and
339 restrict the field of the study. So, it was assumed that the membrane and transmembrane pressure
340 do not alter the characteristics of the suspension and therefore the carotenoid bioaccessibility. This

341 assumption considered the retentions of the main compounds of juices are close to each other for
342 the 4 tested membranes, i.e. retentions are only little affected by fouling, even if it can be a little
343 different from one membrane to another (Dornier et al., 2018; Hofs, Ogier, Vries, Beerendonk, &
344 Cornelissen, 2011). The enzyme mixture effect was restricted in this part because it was not possible
345 to modulate the activity profile and this was not the core of the work. The used process combined an
346 enzymatic treatment in batch mode with the comparison of both pectinolytic mixtures ($300 \mu\text{L}\cdot\text{kg}^{-1}$,
347 45 min, 30°C) and crossflow microfiltration at MRR 1 ($1.8 - 3.5 \text{ bar}$, $1 \text{ m}\cdot\text{s}^{-1}$, 30°C). Thus, for the four
348 membranes, with different TmP and enzymatic treatment, the performance of the operation was
349 assessed measuring permeate flux, J_p , as well as the physico-chemical characteristics of juice in order
350 to select the best membrane/TmP/enzyme combination.

351 - the second phase considered the complete process. It aimed to identify the other operating
352 parameters that most influence carotenoid bioaccessibility, permeate flux and physico-chemical
353 properties of citrus concentrates thanks to a fractional factorial experimental design of Plackett-
354 Burman (Goupy, 2006; Vanaja & Shobha Rani, 2007). The process combined i) an enzymatic
355 liquefaction with the preselected enzyme mixture at $300 \mu\text{L kg}^{-1}$ ii) a crossflow microfiltration
356 operation using the preselected membrane/TmP combination with or without diafiltration, iii) a
357 possible additional step of pasteurization. Seven operating parameters were modulated: enzymatic
358 liquefaction conditions (dose of enzyme, temperature, implementation mode), CMF conditions
359 (crossflow velocity, temperature), and with or without diafiltration and pasteurization alone or in
360 combination (**Table 2**). Statistical analyses were performed from means and standard deviations
361 using XLSTAT software 2016. Statistical significance was tested using one-way analysis of variance
362 with a post-hoc Fisher's test. A P value < 0.05 was considered statically significant. From a Plackett-
363 Burman experimental design, the effects of each factor were calculated by multiple linear regression
364 using MS-Excel between the lowest and the highest level [-1, 1]. Relative effects were obtained
365 dividing them by the mean value (expressed in %).

366 - The last phase aimed to investigate further the process focusing on the most influent operating
367 conditions and considering simultaneously carotenoid bioaccessibility and process performance.

368

369 **3. Results and discussion**

370 **3.0. Initial citrus juice characterization**

371 As a reminder, an initial standardized citrus juice was formulated by mixing clementine and
372 grapefruit juices with a ratio of 60/40% in order to nutritionally optimize the carotenoid profile. So,
373 raw citrus juice was characterized to later assess the effect of processing on the concentrates.
374 Physico-chemical analysis, carotenoid content and bioaccessibility of citrus juices were assessed
375 (**Table 3**). Juice from lot A was used for the first phase, lot B was used for the second and third phase
376 and the last juice from lot C was only used for the third phase. Note that with regard to the physico-
377 chemical and structural parameters, juices from the different lots were very similar whereas their
378 carotenoid content and bioaccessibility differed significantly. The impact of lot appeared greater for
379 carotenoid content and bioaccessibility which were more affected by a possible difference in fruit
380 maturity before processing or by several slight variations in processing between lots.

381

382 *Physico-chemical and structural parameters*

383

384 The pH of citrus juices was acid which facilitates their preservation. A fruit juice is a suspension, i.e. a
385 solid-liquid dispersion. It is a heterogeneous and unstable mixture due to the existence of two
386 phases: the dispersing phase, water with TSS (soluble fraction) and the dispersed phase with SIS
387 (colloidal, supra-colloidal and particulate fractions). The dispersing phase occupies almost all the
388 juice and is mainly composed of carbohydrates and organic acids (Dahdouh, Delalonde, Ricci,
389 Rouquie, & Wisniewski, 2016). Note that TSS was close to that of grapefruit or orange juice (95 and

390 100 g.kg⁻¹ respectively). The average ratio TSS/SIS, which is an essential characteristic for carotenoid
391 purification by CMF, was about 33 (Servent, Abreu, Dhuique-Mayer, Belleville, Dornier, 2020). The SIS
392 corresponded to the pulp in juices and represented the particulate fraction with particle size over
393 100 µm. By the way, the mean volume diameter of citrus juice was high (about 900 µm). Regarding
394 the viscosity, juices behaved as rheofluidifiers with a low viscosity equal to 2-3 mPa.s, which is very
395 close to that of pure water.

396

397 *Carotenoid analysis*

398 Carotenoid content and bioaccessibility were very different for the three carotenoids.
399 Citrus juices contained three main carotenoids where lycopene provided by grapefruit had the
400 highest concentration (in average for lots B and C, 5.55 mg.kg⁻¹) followed by the two provitamin A
401 carotenoids: β-cryptoxanthin (2.85 mg.kg⁻¹) and β-carotene (1.29 mg.kg⁻¹) mainly provided by
402 clementine (**Table 3**). The addition of grapefruit juice to clementine juice resulted in a balanced
403 carotenoid composition by increasing β-carotene and providing lycopene (Poulaert et al., 2012). On
404 the other hand, carotenoid bioaccessibility varied between the three carotenoids in the following
405 order: BCX > BC > LYC. Carotenoid bioaccessibility strongly depends on carotenoid type (carotene or
406 xanthophyll) and this order is in agreement with literature, whatever the food source. Indeed,
407 xanthophylls (BCX), which are less hydrophobic than carotenes, are located at the surface of lipid
408 droplets which means they are released more easily from lipid droplets and therefore, more easily
409 incorporated into mixed micelles (Tyssandier, Lyan, & Borel, 2001). Furthermore, although lycopene
410 content was the highest, its bioaccessibility was the lowest (< 1%). The low bioaccessibility of
411 lycopene could be due to the morphology of chromoplasts. Indeed, a recent study has shown that
412 chromoplasts with crystalline morphology accumulated in red-fleshed grapefruits with an extremely
413 high accumulation of lycopene (96%) (Zhang et al., 2019). Furthermore, fruits with high carotenoid
414 content in crystalline chromoplasts had lower bioaccessibility than the others which accumulated

415 high content of carotenoid in globular chromoplasts (R. M. Schweiggert et al., 2012). Regarding the
416 RAE, the consumption of 250 g of juice provided an average of 55 μg of vitamin A equivalent which
417 corresponds to about 8% of the Recommended Dietary Allowances (RDA). These values were very
418 similar to those obtained with homemade orange juice where RAE was about 43 μg for a glass of 250
419 g, i.e. 5.4% of RDA (Carla M. Stinco et al., 2012) but were considerably less than carrot juice which
420 provides 1690 μg per 250g (211.3% of RDA). Taking into account the bioaccessibility, the RAE* of
421 citrus juice was drastically divided by approximately 5 which corresponds to only 1.8% of the RDA.
422 Finally, RAE overestimates the contribution of vitamin A. It is relevant to take into account
423 carotenoid bioaccessibility to more accurately assess the provitamin A equivalent provided by food.

424

425 **3.1. Selection of enzyme, transmembrane pressure and membrane combination**

426

427 **3.1.1. Influence of enzymatic treatment on permeate flux and structural characteristics of juices**

428

429 *Permeate flux*

430 Stabilized permeate flux obtained during crossflow microfiltration of the untreated citrus juice and
431 the juice previously treated with both commercial enzymes, Ultrazym and Pectinex, are presented in
432 **Table 4**. In all the tested cases, enzymatic liquefaction enhanced the permeate flux. Considering that
433 repeatability of permeate flux measurements using this type of well-controlled pilot equipment is
434 between 5 and 10%, enzyme treatment allowed to increase J_p for the membranes PALL, ORELIS and
435 TAMI significantly (J_p multiplied by 1.17 to 1.54). Except for the ORELIS membrane, the results
436 indicated there was no significant difference in permeate flux between both enzymes. Many studies
437 showed that pectinolytic enzymes such as Ultrazym or Pectinex, thanks to soluble pectin
438 depolymerization and damage to the cell wall polysaccharides, have long been used to decrease
439 viscosity, to limit the fouling power of fruit juices and therefore, to increase filtration performance

440 (Ushikubo, Watanabe, & Viotto, 2007; F. Vaillant et al., 1999; Yu & Lencki, 2004). In addition,
441 Chaparro, Dhuique-Mayer et al. (2016) explained the permeate flux rise by disorganizing the gel-like
442 structure that can be formed at the surface of the membrane, facilitating mass transfers through the
443 porous media. The ST-GOBAIN membrane clearly differed from the others because the flux was not
444 significantly modified after enzyme treatment with this membrane. This variation in behaviour can
445 be linked to a different fouling mechanism of this membrane because, on the one hand, of its larger
446 average pore diameter more favourable to internal fouling (0.6 μm instead of 0.2 μm) and, on the
447 other hand, of the very different nature of the membrane material (silicon carbide instead of metal
448 oxides) which probably did not lead to the same interactions with the product.

449

450 *Physico-chemical and structural parameters*

451 Neither enzymatic liquefaction (whatever mixture is used) nor crossflow microfiltration (30°C, 2.6
452 bar, MRR 1, 5 $\text{m}\cdot\text{s}^{-1}$) modified pH, TSS, AT, TDM, SIS or turbidity (**Table S1**).

453 Particle size spectra comparison (**Figure S1**) showed enzymatic liquefaction drastically decreased the
454 particle volume diameter of citrus juices: $D[4,3]$ was reduced from 6 up to 9 fold (**Figure 2**). Indeed,
455 the particulate fraction ($> 100 \mu\text{m}$) was degraded and replaced by the supra-colloidal fraction (< 100
456 μm). Enzymatic liquefaction with Ultrazym had a stronger effect than with Pectinex on particle size
457 distribution: particle size was 4 fold lower with Ultrazym than with Pectinex. Without using enzymes,
458 it could be observed that the high shear rates during crossflow microfiltration considerably
459 decreased particle size of untreated citrus juice as also shown by Dahdouh et al. (2016) but not as
460 much as enzymatic liquefaction. It was also noted that particle size in the juices that have undergone
461 microfiltration in addition to an enzymatic treatment was similar to those that have undergone only
462 the enzymatic treatment.

463 Regarding particle size dispersion, the span was low for the raw juice mainly characterized by a single
464 peak of large particles ($> 1000 \mu\text{m}$), and increased slightly for microfiltered juice that gave bimodal

465 distribution (two main populations at around 100 and 900 μm). For juices treated with enzymes,
466 either microfiltered or not, the span was higher than untreated juices, characterized by no peak and
467 particle sizes ranging from 5 to 900 μm .

468 Enzymatic liquefaction decreased viscosity by 30% but no significant difference between the two
469 enzymes, Ultrazym and Pectinex, was observed (**Figure 3**). Similar results were found by Vaillant,
470 Millan, O'Brien et al. in passion fruit juice (F. Vaillant et al., 1999). This phenomenon is well known
471 (Kuddus, 2018) and is related to the actions of pectinolytic enzymes on the soluble pectin fraction
472 and also on the pectic compounds entrapped in the cell walls that make up the bulk of suspended
473 insoluble solids. Through hydrolytic cleavage (polygalacturonase activity), non-hydrolytic breakdown
474 (pectin-lyase activity) or deesterification (pectinesterase activity), these enzymes contribute to
475 decrease molar mass of pectins and chemical interactions between biopolymers chains (mainly H-
476 bonds) what leads to a viscosity drop (Jayani, Saxena, & Gupta, 2005) .

477 On the other hand, crossflow microfiltration did not modify either the viscosity of the untreated juice
478 or the viscosity of the juices previously treated with enzymes. Due to the constant MRR (equal to 1),
479 the rheological properties of juice were not much affected by microfiltration. Note that only particle
480 size was modified by microfiltration, suggesting that there was no correlation between particle size
481 distribution and viscosity. Moreover, for a constant MRR, the effect of enzymatic treatment on
482 viscosity was greater than that of microfiltration.

483 Thanks to the degradation of the cell wall polysaccharides, together with that of the soluble pectins,
484 enzymatic treatments considerably modified the physical characteristics of the suspension. Particle
485 size and viscosity of juice were decreased that was, in our case, favorable for mass transfers through
486 the membrane and was conducive to higher permeate fluxes (Ushikubo et al., 2007; F. Vaillant et al.,
487 1999; Yu & Lencki, 2004). Thus, using pectinolytic enzymes is an interesting way to improve process
488 performance.

489

490 **3.1.2. Effect of TMP on permeate flux and structural characteristics of juices pre-liquefied with**
491 **enzymes**

492

493 *Permeate flux*

494

495 The comparison of permeate flux for different transmembrane pressures and membranes was made
496 in a pressure range between 0.8 and 4.3 bar (**Figure 4**). As provided by Darcy's law, at constant MRR,
497 permeate flux increased by increasing the transmembrane pressure that corresponds to the driven
498 force for mass transfers through the porous medium. Nevertheless, permeate flux was not
499 proportional to TmP and, a plateau was reached when TmP increased. So an optimal pressure over
500 which it is not interesting to filtrate the product could be defined (around 3 bar in our case). These
501 results, that could be explained by the increasing hydraulic resistance of the fouled membrane with
502 pressure, are very usual and are in accordance with many studies such as Cisse et al. 2011 (Cisse,
503 Vaillant, Soro, Reynes, & Dornier, 2011) who also have specified that the transmembrane pressure
504 effect varied according to the MRR. The TAMI membrane gave the highest permeate flux under any
505 TmP, followed by ST-GOBAIN and PALL which had similar permeate flux trends and then the ORELIS
506 membrane. These differences between the membrane behavior were surely due to their different
507 structural characteristics (thickness, porosity, tortuosity, pore diameter distribution, surface state)
508 and to the different materials that could be more or less favorable to physico-chemical interactions
509 with juice components. Surprisingly, the ST GOBAIN membrane was not the most effective even if it
510 showed a much higher water permeability than the others and a larger average pore diameter. As
511 often shown in many cases in microfiltration (Cheryan, 1998), this difference could be related to its
512 higher average pore diameter that promotes the internal part of membrane fouling (through pore
513 constriction and/or blocking) and so create a higher hydraulic resistance of the system.

514 From TmP of 3 bar, permeate flux were higher than $100 \text{ kg}\cdot\text{h}^{-1}\cdot\text{m}^{-2}$, for all the membranes, that was
515 an encouraging value for industrial application of the process. TAMI membrane showed promise

516 from an energy point of view because it was able to filtrate at a lower transmembrane pressure while
517 guaranteeing a higher permeate flux.

518

519 *Physico-chemical and structural parameters*

520 As might be expected, transmembrane pressure did not cause any modifications of juice
521 characteristics. Shear stress variations induced by passing through the pressure regulating valve was
522 probably negligible compared to the shear stress generated by high fluid velocity into the circulation
523 loop.

524

525 Finally, TAMI membrane was selected guaranteeing the best permeate flux at low transmembrane
526 pressure. By the way, an average transmembrane pressure of around 2.5 bar was chosen to ensure
527 high filtration performance while maintaining an acceptable energetic cost for the process.

528 Due to the similar effects of the two enzymes on performance filtration, the choice of enzymatic
529 treatment was oriented towards Ultrazym. It further reduced the particle size of juice and low
530 particle size appeared to induce better permeate flux.

531 Having found this enzyme/membrane/transmembrane pressure combination, it is possible to go
532 further with the process and optimize it in order to obtain concentrates with the best carotenoid
533 bioaccessibility and therefore with the highest nutritional qualities.

534

535 **3.2. Selection of the most influential factors on carotenoid bioaccessibility**

536

537 **3.2.1. Process performance and concentrate characteristics**

538 In this part of the study, crossflow microfiltration was carried out concentrating the product in the
539 retentate loop up to a MRR of 4.4.

540

541 *Permeate flux*

542 Results showed permeate flux varied from 15 to 120 kg.h⁻¹.m⁻². It was logically the lowest for the C8
543 concentrate that was the least treated concentrate (no enzymatic liquefaction, no diafiltration, low
544 crossflow velocity and filtration temperature) contrary to the C4 concentrate (**Table 5**). Regarding the
545 stability of permeate flux, the C8 concentrate appeared to be the one with the most stable permeate
546 flux, followed by C1 and C2. The higher stability of permeate flux observed with the concentrate C8,
547 could be related to the softer operating conditions used (low temperature and crossflow velocity, no
548 enzyme treatment) and to the low permeate flux that could favor a more progressive fouling of the
549 membrane during the concentration. On the contrary, C3, C5, C6 were characterized by a high
550 coefficient of instability $\partial J_p / \partial MRR$. No correlation between permeate flux and stability was
551 observed. Of course, the higher and more stable the permeate flux the better the process for
552 industrial application (cf. some examples **Figure S2**).

553

554 *Physico-chemical and structural parameters*

555

556 Several parameters were evaluated in juice and in the 8 concentrates at MRR 4.3 (Table 5). Firstly,
557 insoluble solids were completely retained by the membrane and increased about 4-fold in
558 concentrates compared to the juice, that is logically close to the MRR attained. Turbidity values were
559 also multiplied by 4 in concentrates, which was in line with a study by Vaillant et al. 2008, which
560 showed that in certain cases, turbidity appears to be a good SIS substitute (Fabrice Vaillant, Pérez,
561 Acosta, & Dornier, 2008). To purify the micronutrients, a step of diafiltration was added following
562 crossflow microfiltration for four concentrates (C2, C4, C5, C6). As expected, declines of TSS and so

563 dry matter (DM) were observed during the diafiltration because the membrane did not retain solutes
564 such as sugars and organic acids.

565 Particle size distribution and viscosity of the 8 concentrates varied and two groups could be
566 distinguished: C1, C4, C6, C7 had a mean volume diameter $D[4,3]$, between 59 and 98 μm and a limit
567 viscosity of 3 mPa.s, whereas the $D[4,3]$ of the concentrates C2, C3, C5 and C8 was between 178 and
568 246 μm with a limit viscosity of 13.5 mPa.s. The difference between these two groups was mainly
569 explained by the enzymatic treatment which led to a decrease in particle size and viscosity.

570

571 *Carotenoid analysis*

572

573 Nutritional quality was assessed for the 8 concentrates, in two dimensions: carotenoid content and
574 carotenoid bioaccessibility (**Figure 5**). For an MRR equal to about 4, crossflow microfiltration mainly
575 and logically increased carotenoid content 4 fold, even if a larger dispersion of lycopene content was
576 observed between concentrates. This dispersion could be due to processing. Indeed, the application
577 of high temperatures, the exposure to light or oxygen could induce the decrease of total lycopene or
578 its isomerization into isomers such as 5 *cis*, 9 *cis*, 13 *cis* and 15 *cis* (Cooperstone, Francis, & Schwartz,
579 2016; Urbanoviciene, Bobinaite, Bobinas, & Viskelis, 2017). The high sensitivity to lycopene
580 isomerization could explain dispersion (Honest, Zhang, & Zhang, 2011; Petry & Mercadante, 2017)
581 where all *cis*-isomers appearing from processing contributed to the variation observed in lycopene
582 quantification. Indeed, the percentage of *cis*-isomers from lycopene varied from 1.7% (C8
583 concentrate) to 9.9% (C1 concentrate) for the eight concentrates. The lowest value was obtained for
584 C8 that was the concentrate treated with the mildest conditions (no enzyme treatment, low
585 temperature, low crossflow velocity and no pasteurization). Furthermore, the process induced
586 carotenoid bioaccessibility changes in the concentrates depending on the combination of operating
587 parameters. Indeed, bioaccessibility varied from 15 to 27% for BC, from 20 to 30% for BCX and from
588 0.6 to 1.5% for LYC. These changes were greater for β -cryptoxanthin and β -carotene bioaccessibility

589 than lycopene bioaccessibility. We can notice that the very low lycopene bioaccessibility for all
590 concentrates did not allow to quantify bioaccessible cis-isomers. So, for lycopene, the cis-
591 isomerization did not affect the bioaccessibility. In fact, the C5 concentrate differed from the others
592 by having the highest BCX and BC bioaccessibility. However, the conditions for obtaining the best
593 carotenoid bioaccessibility were not the same as those that gave the best filtration performance
594 (high and stable J_p). So a compromise will have to be found between carotenoid bioaccessibility and
595 filtration performance.

596

597 *Vitamin A activity*

598 RAE and RAE* were calculated to assess vitamin A delivered by juice and the 8 concentrates.

599 Of course, crossflow microfiltration induced an increase of RAE by 4 because of the carotenoid
600 content which was multiplied by 4 by CMF. A portion of 250 g of concentrate provided from 30 to 36
601 % of RDA, depending on the concentrate. Taking into account the bioaccessibility, RAE* values of
602 concentrates were divided by up to 4.5, as for juices, and provided from 6 to 10 % of RDA. For
603 concentrates, it should be noted that the dispersion of the RAE* was greater than the RAE, which
604 may be explained by a more variable process effect on bioaccessibility than on the carotenoid
605 content alone between concentrates. In fact, although taking into account the fact that
606 bioaccessibility decreased vitamin A intake, microfiltration compensated this decrease and even
607 increased it. Indeed, 250 g of juice provided 1.8 % RDA, whereas after microfiltration, 250 g of
608 concentrate provided up to 10% of RDA (for C5 concentrate). Note that the RAE* was probably
609 underestimated because it was calculated from RAE which was theoretically defined by IOM and
610 already takes into account the bioefficacy of carotenoids (West, Eilander, & van Lieshout, 2002).

611

612 **3.2.2. Effects of the operating conditions on permeate flux and concentrate quality**

613 *Permeate flux and stability*

614

615 The three most influential parameters on permeate flux have positive effects on it. The importance
616 of their effects was in descending order enzyme dose (84%), filtration temperature T_{CMF} (50%) and
617 crossflow velocity U (45%). These 3 parameters alone explained almost 90% of the cumulated effect
618 of all operating parameters thanks to a decrease in viscosity and membrane fouling. The other
619 parameters, liquefaction temperature and mode (T_{liq} and M_{liq}), as well as diafiltration, did not have a
620 significant effect on permeate flux (2.6%, 2.1% and 1.6% respectively). This last observation is not in
621 accordance with literature where usually the diafiltration step increases J_p slightly. Indeed, feeding
622 with water instead of juice decreases the viscosity and contributes to enhancing permeate flux
623 according to Darcy's law (Basso, Gonçalves, Grimaldi, & Viotto, 2009; Polidori et al., 2018). In this
624 work, diafiltration had no effect on permeate flux probably because the diavolume ratio of 1.0 was
625 too low and the diafiltration was carried out at the end of the microfiltration, when the MRR of 4.4
626 was already attained.

627 The three most influential parameters on permeate flux stability were little different from the three
628 most influential parameters on permeate flux. There were in descending order the liquefaction
629 temperature T_{liq} (112.9%), the crossflow velocity U (40.7%) and filtration temperature T_{CMF} (24.0%).
630 Liquefaction temperature accounted for almost 50% of the cumulated effect of all the operating
631 parameters. In addition, contrary to the permeate flux, crossflow velocity (U) and filtration
632 temperature (T_{CMF}) had a negative effect on stability and thus decreased it. Enzymatic treatment had
633 no effect on permeate flux stability (4.6%), whereas it drastically increased permeate flux.

634

635 *Concentrate characteristics*

636 Pareto charts were used to highlight the relative importance of the seven operating parameter
637 effects on nutritional and structural qualities of concentrates (**Figures 6 and 7**). These charts were
638 made up of two axes: the abscissa axis was the causes (operating parameters) and the ordinate axis
639 was the effect on the response studied (carotenoid bioaccessibility and structural parameters). The

640 orange curve corresponded to cumulated percentage. Significance threshold could not be
641 determined statistically because of the cumbersome experimental procedure which did not allow to
642 repeat each trials 3 times. Nevertheless, we considered effects below 10% insignificant because of
643 the same order of magnitude as the repeatability.

644 Enzyme treatment parameters (dose, temperature T_{liq} and mode M_{liq}) were the most influential
645 operating parameters on pro-vitamin A carotenoid bioaccessibility (BC and BCX) (**Figure 6**). T_{liq} and
646 M_{liq} had a positive effect whereas the dose had a negative effect on pro-vitamin A carotenoid
647 bioaccessibility. It was quite different for lycopene bioaccessibility, which was mainly influenced by
648 enzyme dose, filtration temperature (T_{CMF}) and crossflow velocity (U) where dose and T_{CMF} had a
649 negative effect whereas crossflow velocity had a positive effect (**Figure 6**). The operating conditions
650 related to the microfiltration, T_{CMF} and U, had a greater impact on the lycopene bioaccessibility than
651 pro-vitamin A carotenoids. This could be due to the greater sensitivity of lycopene to isomerization
652 and oxidation during food processing (Cooperstone et al., 2016; Urbanoviciene et al., 2017). Note
653 that contrary to our results, recent studies on tomato showed that thermal processing can improve
654 the lycopene bioaccessibility (Colle, Lemmens, Van Buggenhout, Van Loey, & Hendrickx, 2010;
655 Knockaert, Pulissery, et al., 2012). The high shear rate caused by high crossflow velocity during
656 crossflow microfiltration contributed to cell breakdown and therefore to the more effective release
657 of crystalloid lycopene from chromoplasts and lycopene bioaccessibility (R. M. Schweiggert et al.,
658 2012).

659 Enzyme dose remained the common cause of decreasing in carotenoid bioaccessibility. The
660 enzymatic treatment led to the modification of pectin concentration and structural properties which
661 could promote its interaction with bile salts. Indeed, Cervantes-Paz et al. (2017) explained the
662 possible interaction of low pectin concentration with bile salts can modulate carotenoid
663 bioaccessibility knowing that bile salts are key components of lipid digestion and micelle formation
664 (Cervantes-Paz et al., 2016). For the three carotenoids, pasteurization did not affect carotenoid
665 bioaccessibility which is in accordance with Sentandreu et al. (2020). Even if it appeared significant

666 for β -carotene, the effect of diafiltration on carotenoid bioaccessibility stayed quiet low. The ability
667 of carotenoids to be incorporated into the micelles depended little or not at all on the major solute
668 fraction. So the step of diafiltration could be interesting to reduce sugar content and therefore to
669 produce healthier concentrates.

670

671 Enzyme dose was the largest cause of decrease of D[4,3] and viscosity which account for 60% and
672 80% respectively of all operating parameters (**Figure 7**). The diafiltration step also contributed to
673 decreasing particle size and viscosity with an effect of over 20%. None of the other parameters had
674 any effect on the structural characteristics studied.

675 Finally, enzyme dose was clearly the most influential parameter on assessed values resulting in a
676 decrease of carotenoid bioaccessibility, particle size and viscosity and in an increase of permeate flux.
677 On the other hand, no correlation between particle size (D[4,3]), viscosity (η) and bioaccessibility was
678 highlighted, confirming results mentioned by Gence. L et al. (Laura Gence, Servent, Poucheret, Hiol,
679 & Dhuique-Mayer, 2016). These observations were contradictory to literature on citrus juices which
680 indicates that the particle size are strongly linked to carotenoid bioaccessibility (Carla M. Stinco et al.,
681 2012). However, concentrates with high J_p were characterized by low viscosity and low particle size.
682 So, a compromise of enzyme dose would be found to ensure the best carotenoid bioaccessibility
683 while maintaining an acceptable performance for the process. Moreover, the other parameters
684 would be selected in order to give the best carotenoid bioaccessibility (enzyme liquefaction in batch
685 mode at 50°C, $T_{CMF} = 30^\circ\text{C}$, $U = 5 \text{ m}\cdot\text{s}^{-1}$, with diafiltration and no pasteurization).

686

687 **3.3. Focus on the most influential factor**

688 The last phase aimed to complete the study of the impact of enzyme dose in order to investigate if it
689 is possible to ensure good carotenoid bioaccessibility while maintaining acceptable process
690 performance. For that, a concentrate was produced at MMR 4.4 fixing the best combination of

691 operating conditions for carotenoid bioaccessibility (based on the results obtained from the Plackett-
692 Burman experimental design in the previous phase) and decreasing Ultrazym dose to $50 \mu\text{L.kg}^{-1}$. So
693 two trials were carried out with the third lot of juice (lot C) using the production of a concentrate
694 without enzymes as a reference (**Table 6**).

695 A pre-liquefaction with a dose of $50 \mu\text{L.kg}^{-1}$ of Ultrazym doubled permeate flux. Thanks to this
696 enzyme treatment, J_p remained above $80 \text{ g.h}^{-1}.\text{m}^{-2}$ up to a MRR of 4.4. This low dose of enzyme was
697 sufficient to ensure high process performance. Furthermore, the permeate flux was very stable for
698 the enzyme treated concentrate compared to the untreated one.

699 The differences of TSS, SIS and DM between the two concentrates were significant ($p < 0.05$) but very
700 slight. The enzymatic treatment with $50 \mu\text{L.kg}^{-1}$ had the same effect on the viscosity as with 300
701 $\mu\text{L.kg}^{-1}$: the viscosity was divided by 3 until it reached a value below 3 mPa.s. Regarding particle size,
702 $50 \mu\text{L.kg}^{-1}$ of Ultrazym modified neither the D[4,3] nor the size dispersion (Span) in the concentrate
703 contrary to the treatment with $300 \mu\text{L.kg}^{-1}$.

704 In this case, carotenoid bioaccessibility was not affected by enzymatic treatment which differs from
705 previous results that showed enzymatic treatment with $300 \mu\text{L.kg}^{-1}$ of Ultrazym was the main cause
706 of the decrease in bioaccessibility of β -carotene, β -cryptoxanthin and lycopene. With $50 \mu\text{L.kg}^{-1}$ of
707 Ultrazym, carotenoid bioaccessibility was preserved and therefore, the RAE* also.

708 The bioaccessibility ratio between initial juices and concentrates, calculated from the 2 main
709 bioaccessible carotenoids (BC and BCX), could be used to compare the last concentrate (with enzyme
710 Table 6) with the C5 concentrate which gave the best bioaccessibilities in the previous part (Table 5).
711 By calculating this ratio, we showed the average bioaccessibility was increased by about 30% in both
712 cases. So the effect of the process on the bioaccessibility of the 2 main carotenoids could be
713 considered as similar.

714 Finally, the final concentrate treated with $50 \mu\text{L.kg}^{-1}$ of enzymes gave high permeate flux with good
715 carotenoid bioaccessibility. So this enzymatic treatment resulted in an interesting compromise

716 between process performance and nutritional quality. Further investigations should be considered to
717 refine the optimization of the enzyme dose and also to provide insights for a better understanding of
718 the phenomena involved.

719

720 **4. Conclusion**

721

722 In this study, a new process based on crossflow microfiltration was investigated by selecting the
723 operating conditions giving the best nutritional quality of the final concentrate evaluated through its
724 carotenoid potential while guaranteeing a high process performance. Among all the operating
725 conditions, the enzyme dose appeared to play a major role on both permeate flux and carotenoid
726 bioaccessibility in the studied process. Several perspectives could be considered to try to better
727 understand these results such as examining in more detail the impact of pectin structure on
728 carotenoid micellarization or what happens at the cellular level after enzymatic treatment. Other
729 enzymes could also be investigated to compare their effects on cellular structure and to explain the
730 variation of carotenoid bioaccessibility.

731 Results showed that bioaccessible carotenoid content could be multiplied by 4.5 to 4.8 in the
732 concentrate in comparison with Citrus juice using CMF up to MRR 4.4. Crossflow microfiltration could
733 be easily carried out up to a higher MRR in that case (high permeate flux and no drastic drop vs.
734 MRR) and so the bioaccessible carotenoid content should be easily increased leading to higher
735 nutritional potential of concentrate. In addition, the coupling of microfiltration with other
736 mechanical processes that could favor cell destructuring/destroying and thus carotenoid release
737 from chromoplasts such as homogenization, would be another avenue of research.

738

739 **Acknowledgements**

740 This work was carried out with the financial support of the Centre for International Cooperation in
741 Agronomic Research for development (CIRAD) and the Doctoral School GAIA (Montpellier, France).

742

743 **Declaration of interests**

744 The authors of this work declare no conflict of interest.

745

746

747 **References**

- 748 Aschoff, J., Rolke, C., Breusing, N., Bosity-Westphal, A., Högel, J., Carle, R., & Schweiggert, R. (2015).
749 Bioavailability of β -cryptoxanthin is greater from pasteurized orange juice than from fresh
750 oranges – a randomized cross-over study. *Molecular nutrition & food research*, 59.
751 doi:10.1002/mnfr.201500327
- 752 Aschoff, J. K., Kaufmann, S., Kalkan, O., Neidhart, S., Carle, R., & Schweiggert, R. M. (2015). In Vitro
753 Bioaccessibility of Carotenoids, Flavonoids, and Vitamin C from Differently Processed
754 Oranges and Orange Juices [Citrus sinensis (L.) Osbeck]. *Journal of Agricultural and Food
755 Chemistry*, 63(2), 578-587. doi:10.1021/jf505297t
- 756 Barba, F. J., Saraiva, J. M. A., Cravotto, G., & Lorenzo, J. M. (2019). *Innovative Thermal and Non-
757 Thermal Processing, Bioaccessibility and Bioavailability of Nutrients and Bioactive
758 Compounds*: Woodhead Publishing.
- 759 Basso, R. C., Gonçalves, L. A. G., Grimaldi, R., & Viotto, L. A. (2009). Degumming and production of
760 soy lecithin, and the cleaning of a ceramic membrane used in the ultrafiltration and
761 diafiltration of crude soybean oil. *Journal of Membrane Science*, 330(1), 127-134.
762 doi:https://doi.org/10.1016/j.memsci.2008.12.052
- 763 Bungau, S., Abdel-Daim, M. M., Tit, D. M., Ghanem, E., Sato, S., Maruyama-Inoue, M., . . .
764 Kadonosono, K. (2019). Health benefits of polyphenols and carotenoids in age-related eye
765 diseases. *Oxidative medicine and cellular longevity*, 2019.
- 766 Cervantes-Paz, B., de Jesús Ornelas-Paz, J., Pérez-Martínez, J. D., Reyes-Hernández, J., Zamudio-
767 Flores, P. B., Rios-Velasco, C., . . . Ruiz-Cruz, S. (2016). Effect of pectin concentration and
768 properties on digestive events involved on micellarization of free and esterified carotenoids.
769 *Food Hydrocolloids*, 60, 580-588.
- 770 Cervantes-Paz, B., Ornelas-Paz, J. d. J., Ruiz-Cruz, S., Rios-Velasco, C., Ibarra-Junquera, V., Yahia, E. M.,
771 & Gardea-Béjar, A. A. (2017). Effects of pectin on lipid digestion and possible implications for
772 carotenoid bioavailability during pre-absorptive stages: A review. *Food Research
773 International*, 99, 917-927. doi:https://doi.org/10.1016/j.foodres.2017.02.012
- 774 Chaparro, L., Dhuique-Mayer, C., Castillo, S., Vaillant, F., Servent, A., & Dornier, M. (2016).
775 Concentration and purification of lycopene from watermelon juice by integrated
776 microfiltration-based processes. *Innovative Food Science & Emerging Technologies*, 37, 153-
777 160. doi:10.1016/j.ifset.2016.08.001
- 778 Cheryan, M. (1998). Ultrafiltration and microfiltration handbook, Technomic Pub. Co., Lancaster, PA.
- 779 Cilla, A., Alegría, A., de Ancos, B. a., Sánchez-Moreno, C. n., Cano, M. P., Plaza, L., . . . Barberá, R.
780 (2012). Bioaccessibility of tocopherols, carotenoids, and ascorbic acid from milk-and soy-
781 based fruit beverages: influence of food matrix and processing. *Journal of Agricultural and
782 Food Chemistry*, 60(29), 7282-7290.
- 783 Cisse, M., Vaillant, F., Soro, D., Reynes, M., & Dornier, M. (2011). Crossflow microfiltration for the
784 cold stabilization of roselle (*Hibiscus sabdariffa* L.) extract. *Journal of Food Engineering*,
785 106(1), 20-27.
- 786 Colle, I., Lemmens, L., Van Buggenhout, S., Van Loey, A., & Hendrickx, M. (2010). Effect of thermal
787 processing on the degradation, isomerization, and bioaccessibility of lycopene in tomato
788 pulp. *Journal of Food Science*, 75(9), C753-C759.
- 789 Cooperstone, J. L., Francis, D. M., & Schwartz, S. J. (2016). Thermal processing differentially affects
790 lycopene and other carotenoids in cis-lycopene containing, tangerine tomatoes. *Food
791 Chemistry*, 210, 466-472. doi:https://doi.org/10.1016/j.foodchem.2016.04.078
- 792 Corredig, M., Kerr, W., & Wicker, L. (2001). Particle size distribution of orange juice cloud after
793 addition of sensitized pectin. *Journal of Agricultural and Food Chemistry*, 49(5), 2523-2526.
- 794 Dahdouh, L., Delalonde, M., Ricci, J., Rouquie, C., & Wisniewski, C. (2016). *Effect of high shear rates
795 on physico-chemical characteristics, rheological behavior and fouling propensity of orange
796 juices during cross-flow microfiltration*.
- 797 Dahdouh, L., Delalonde, M., Ricci, J., Ruiz, E., & Wisniewski, C. (2018). Influence of high shear rate on
798 particles size, rheological behavior and fouling propensity of fruit juices during crossflow

799 microfiltration: Case of orange juice. *Innovative Food Science & Emerging Technologies*, *48*,
800 304-312. doi:<https://doi.org/10.1016/j.ifset.2018.07.006>

801 Dahdouh, L., Wisniewski, C., Ricci, J., Kapitan-Gnimdu, A., Dornier, M., & Delalonde, M. (2015).
802 Development of an original lab-scale filtration strategy for the prediction of microfiltration
803 performance: Application to orange juice clarification. *Separation and Purification*
804 *Technology*, *156*, 42-50. doi:<https://doi.org/10.1016/j.seppur.2015.10.010>

805 de Abreu, F. P., Dornier, M., Dionisio, A. P., Carail, M., Caris-Veyrat, C., & Dhuique-Mayer, C. (2013).
806 Cashew apple (*Anacardium occidentale* L.) extract from by-product of juice processing: a
807 focus on carotenoids. *Food Chem*, *138*(1), 25-31. doi:10.1016/j.foodchem.2012.10.028

808 Dhuique-Mayer, C., Borel, P., Reboul, E., Caporiccio, B., Besancon, P., & Amiot, M. J. (2007). β -
809 Cryptoxanthin from Citrus juices: Assessment of bioaccessibility using an in vitro
810 digestion/Caco-2 cell culture model. *The British journal of nutrition*, *97*, 883-890.
811 doi:10.1017/S0007114507670822

812 Dornier, M., Belleville, M.-P., & Vaillant, F. (2018). Membrane Technologies for Fruit Juice Processing.
813 In A. Rosenthal, R. Deliza, J. Welti-Chanes, & G. V. Barbosa-Cánovas (Eds.), *Fruit Preservation:
814 Novel and Conventional Technologies* (pp. 211-248). New York, NY: Springer New York.

815 Etcheverry, P., Grusak, M. A., & Fleige, L. E. (2012). Application of in vitro bioaccessibility and
816 bioavailability methods for calcium, carotenoids, folate, iron, magnesium, polyphenols, zinc,
817 and vitamins B6, B12, D, and E. *Frontiers in physiology*, *3*, 317.

818 Gates, K. W. (2012). Essentials of Thermal Processing by Gary S. Tucker and Susan Featherstone.
819 *Journal of Aquatic Food Product Technology*, *21*(4), 393-400.
820 doi:10.1080/10498850.2012.692660

821 Gence, L., Servent, A., Poucheret, P., Hiol, A., & Dhuique-Mayer, C. (2016). *Citrus juices vs*
822 *concentrates obtained by innovative membrane technology: Bioaccessibility of pro-vitamin A*
823 *carotenoids*.

824 Gence, L., Servent, A., Poucheret, P., Hiol, A., & Dhuique-Mayer, C. (2018). Pectin structure and
825 particle size modify carotenoid bioaccessibility and uptake by Caco-2 cells in citrus juices vs.
826 concentrates. *Food Funct*, *9*(6), 3523-3531. doi:10.1039/c8fo00111a

827 Gies, M., Descalzo, A. M., Servent, A., & Dhuique-Mayer, C. (2019). Incorporation and stability of
828 carotenoids in a functional fermented maize yogurt-like product containing phytosterols.
829 *Lwt*, *111*, 105-110.

830 Gleize, B., Steib, M., André, M., & Reboul, E. (2012). Simple and fast HPLC method for simultaneous
831 determination of retinol, tocopherols, coenzyme Q10 and carotenoids in complex samples.
832 *Food Chemistry*, *134*(4), 2560-2564. doi:<https://doi.org/10.1016/j.foodchem.2012.04.043>

833 Goupy, J. (2006). *Plans d'expériences*: Ed. Techniques Ingénieur.

834 Hofs, B., Ogier, J., Vries, D., Beerendonk, E. F., & Cornelissen, E. R. (2011). Comparison of ceramic and
835 polymeric membrane permeability and fouling using surface water. *Separation and*
836 *Purification Technology*, *79*(3), 365-374.

837 Honest, K. N., Zhang, H. W., & Zhang, L. (2011). Lycopene: Isomerization Effects on Bioavailability and
838 Bioactivity Properties. *Food Reviews International*, *27*(3), 248-258.
839 doi:10.1080/87559129.2011.563392

840 Jayani, R. S., Saxena, S., & Gupta, R. (2005). Microbial pectinolytic enzymes: a review. *Process*
841 *Biochemistry*, *40*(9), 2931-2944.

842 Knockaert, G., Lemmens, L., Van Buggenhout, S., Hendrickx, M., & Van Loey, A. (2012). Changes in β -
843 carotene bioaccessibility and concentration during processing of carrot puree. *Food*
844 *Chemistry*, *133*(1), 60-67. doi:<https://doi.org/10.1016/j.foodchem.2011.12.066>

845 Knockaert, G., Pulissery, S. K., Colle, I., Van Buggenhout, S., Hendrickx, M., & Van Loey, A. (2012).
846 Lycopene degradation, isomerization and in vitro bioaccessibility in high pressure
847 homogenized tomato puree containing oil: Effect of additional thermal and high pressure
848 processing. *Food Chemistry*, *135*(3), 1290-1297.

849 Kopec, R. E., & Failla, M. L. (2018). Recent advances in the bioaccessibility and bioavailability of
850 carotenoids and effects of other dietary lipophiles. *Journal of Food Composition and Analysis*,
851 68, 16-30. doi:https://doi.org/10.1016/j.jfca.2017.06.008

852 Kuddus, M. (2018). *Enzymes in food biotechnology: production, applications, and future prospects*:
853 Academic Press.

854 Lee, Y., Hu, S., Park, Y.-K., & Lee, J.-Y. (2019). Health Benefits of Carotenoids: A Role of Carotenoids in
855 the Prevention of Non-Alcoholic Fatty Liver Disease. *Preventive nutrition and food science*,
856 24(2), 103.

857 Lemmens, L., Van Buggenhout, S., Oey, I., Van Loey, A., & Hendrickx, M. (2009). Towards a better
858 understanding of the relationship between the β -carotene in vitro bio-accessibility and
859 pectin structural changes: a case study on carrots. *Food Research International*, 42(9), 1323-
860 1330.

861 Macedo, M., Robrigues, R. D. P., Pinto, G. A. S., & de Brito, E. S. (2015). Influence of pectinolytic and
862 cellulolytic enzyme complexes on cashew bagasse maceration in order to obtain carotenoids.
863 *Journal of Food Science and Technology*, 52(6), 3689-3693. doi:10.1007/s13197-014-1411-x

864 Maktouf, S., Neifar, M., Drira, S. J., Baklouti, S., Fendri, M., & Châabouni, S. E. (2014). Lemon juice
865 clarification using fungal pectinolytic enzymes coupled to membrane ultrafiltration. *Food and*
866 *Bioproducts Processing*, 92(1), 14-19.

867 Medicine, I. o. (2001). *Dietary Reference Intakes for Vitamin A, Vitamin K, Arsenic, Boron, Chromium,*
868 *Copper, Iodine, Iron, Manganese, Molybdenum, Nickel, Silicon, Vanadium, and Zinc.*
869 Washington, DC: The National Academies Press.

870 Mierczynska-Vasilev, A., & Smith, P. (2015). Current state of knowledge and challenges in wine
871 clarification. *Australian journal of grape and wine research*, 21, 615-626.

872 Petry, F. C., & Mercadante, A. Z. (2017). Impact of in vitro digestion phases on the stability and
873 bioaccessibility of carotenoids and their esters in mandarin pulps. *Food & Function*, 8(11),
874 3951-3963. doi:10.1039/C7FO01075C

875 Polidori, J., Dhuique-Mayer, C., & Dornier, M. (2018). Crossflow microfiltration coupled with
876 diafiltration to concentrate and purify carotenoids and flavonoids from citrus juices.
877 *Innovative Food Science & Emerging Technologies*, 45, 320-329.
878 doi:https://doi.org/10.1016/j.ifset.2017.11.015

879 Poulaert, M., Borel, P., Caporiccio, B., Gunata, Z., & Dhuique-Mayer, C. (2012). Grapefruit Juices
880 Impair the Bioaccessibility of β -Carotene from Orange-Fleshed Sweet Potato but Not Its
881 Intestinal Uptake by Caco-2 Cells. *Journal of Agricultural and Food Chemistry*, 60(2), 685-691.
882 doi:10.1021/jf204004c

883 Rodriguez-Concepcion, M., Avalos, J., Bonet, M. L., Boronat, A., Gomez-Gomez, L., Hornero-Mendez,
884 D., . . . Zhu, C. (2018). A global perspective on carotenoids: Metabolism, biotechnology, and
885 benefits for nutrition and health. *Progress in Lipid Research*, 70, 62-93.
886 doi:https://doi.org/10.1016/j.plipres.2018.04.004

887 Schweiggert, R., & Carle, R. (2017). Carotenoid deposition in plant and animal foods and its impact on
888 bioavailability. *Critical Reviews in Food Science and Nutrition*, 57(9), 1807-1830.

889 Schweiggert, R. M., Mezger, D., Schimpf, F., Steingass, C. B., & Carle, R. (2012). Influence of
890 chromoplast morphology on carotenoid bioaccessibility of carrot, mango, papaya, and
891 tomato. *Food Chemistry*, 135(4), 2736-2742.

892 Sentandreu, E., Stinco, C. M., Vicario, I. M., Mapelli-Brahm, P., Navarro, J. L., & Meléndez-Martínez,
893 A. J. (2020). High-pressure homogenization as compared to pasteurization as a sustainable
894 approach to obtain mandarin juices with improved bioaccessibility of carotenoids and
895 flavonoids. *Journal of Cleaner Production*, 262, 121325.
896 doi:https://doi.org/10.1016/j.jclepro.2020.121325

897 Servent, A., Abreu, F. A. P., Dhuique-Mayer, C., Belleville, M. P., & Dornier, M. (2020). Concentration
898 and purification by crossflow microfiltration with diafiltration of carotenoids from a by-
899 product of cashew apple juice processing. *Innovative Food Science and Emerging*
900 *Technologies*, 66, 102519.

- 901 Stinco, C. M., Fernández-Vázquez, R., Escudero-Gilete, M. L., Heredia, F. J., Meléndez-Martínez, A. J.,
 902 & Vicario, I. M. (2012). Effect of Orange Juice's Processing on the Color, Particle Size, and
 903 Bioaccessibility of Carotenoids. *Journal of Agricultural and Food Chemistry*, 60(6), 1447-1455.
 904 doi:10.1021/jf2043949
- 905 Stinco, C. M., Pumilia, G., Giuffrida, D., Dugo, G., Meléndez-Martínez, A. J., & Vicario, I. M. (2019).
 906 Bioaccessibility of carotenoids, vitamin A and α -tocopherol, from commercial milk-fruit juice
 907 beverages: contribution to the recommended daily intake. *Journal of Food Composition and*
 908 *Analysis*, 78, 24-32.
- 909 Sun, Y., Tao, W., Huang, H., Ye, X., & Sun, P. (2019). Flavonoids, phenolic acids, carotenoids and
 910 antioxidant activity of fresh eating citrus fruits, using the coupled in vitro digestion and
 911 human intestinal HepG2 cells model. *Food Chemistry*, 279, 321-327.
 912 doi:https://doi.org/10.1016/j.foodchem.2018.12.019
- 913 Tyssandier, V., Lyan, B., & Borel, P. (2001). Main factors governing the transfer of carotenoids from
 914 emulsion lipid droplets to micelles. *Biochimica et Biophysica Acta (BBA) - Molecular and Cell*
 915 *Biology of Lipids*, 1533(3), 285-292. doi:https://doi.org/10.1016/S1388-1981(01)00163-9
- 916 Urbanoviciene, D., Bobinaite, R., Bobinas, C., & Viskelis, P. (2017). *Stability and isomerisation of*
 917 *lycopene in oil-based model system during accelerated shelf-life testing*. Paper presented at
 918 the 11th Baltic Conference on Food Science and Technology" Food science and technology in
 919 a changing world" FOODBALT 2017, Jelgava, Latvia, 27-28 April 2017.
- 920 Ushikubo, F. Y., Watanabe, A. P., & Viotto, L. A. (2007). Microfiltration of umbu (*Spondias tuberosa*
 921 Arr. Cam.) juice. *Journal of Membrane Science*, 288(1-2), 61-66.
- 922 Vaillant, F., Millan, P., O'Brien, G., Dornier, M., Decloux, M., & Reynes, M. (1999). Crossflow
 923 microfiltration of passion fruit juice after partial enzymatic liquefaction. *Journal of Food*
 924 *Engineering*, 42(4), 215-224. doi:https://doi.org/10.1016/S0260-8774(99)00124-7
- 925 Vaillant, F., Pérez, A. M., Acosta, O., & Dornier, M. (2008). Turbidity of pulpy fruit juice: A key factor
 926 for predicting cross-flow microfiltration performance. *Journal of Membrane Science*, 325(1),
 927 404-412.
- 928 Vanaja, K., & Shobha Rani, R. (2007). Design of experiments: concept and applications of Plackett
 929 Burman design. *Clinical research and regulatory affairs*, 24(1), 1-23.
- 930 West, C. E., Eilander, A., & van Lieshout, M. (2002). Consequences of revised estimates of carotenoid
 931 bioefficacy for dietary control of vitamin A deficiency in developing countries. *The Journal of*
 932 *nutrition*, 132(9), 2920S-2926S.
- 933 Yu, J., & Lencki, R. (2004). Effect of enzyme treatments on the fouling behavior of apple juice during
 934 microfiltration. *Journal of Food Engineering*, 63(4), 413-423.
- 935 Zhang, Y., Liu, Y., Liu, F., Zheng, X., Xie, Z., Ye, J., . . . Zeng, Y. (2019). Investigation of chromoplast
 936 ultrastructure and tissue-specific accumulation of carotenoids in citrus flesh. *Scientia*
 937 *Horticulturae*, 256, 108547. doi:https://doi.org/10.1016/j.scienta.2019.108547

938

939 **Figure captions**

940 **Figure 1.** Process flow diagram of the experimental setup (see abbreviation list for meanings).

941 **Figure 2.** Effect of crossflow microfiltration ($T_{CMF} = 30^{\circ}\text{C}$, $U = 5 \text{ m}\cdot\text{s}^{-1}$, $TmP = 2.6 \text{ bar}$, obtained at $MRR =$
 942 1 with the 4 membranes mounted in series) and enzymatic treatment ($300 \mu\text{L}\cdot\text{kg}^{-1}$, $t_{liq} = 90 \text{ min}$, $T_{liq} =$
 943 30°C , $M_{liq} = \text{batch}$) on the mean volume diameter $D[4,3]$ and span of particles in the products: raw
 944 Juice (Lot A), enzyme treated juices with Ultrazym (Juice-Ult) and Pectinex (Juice-Pec), retentates of

945 microfiltration without enzyme (Juice CMF), with enzyme treatments (Juice-Ult CMF and Juice-Pec
946 CMF). Values with the same letters were not significantly different at $p < 0.05$.

947 **Figure 3.** Effect of crossflow microfiltration ($T_{CMF} = 30^{\circ}\text{C}$, $U = 5 \text{ m}\cdot\text{s}^{-1}$, $T_{mP} = 2.6 \text{ bar}$, obtained at MRR
948 $= 1$ with the 4 membranes mounted in series) and enzymatic treatment ($300 \mu\text{L}\cdot\text{kg}^{-1}$, $t_{liq} = 90 \text{ min}$, T_{liq}
949 $= 30^{\circ}\text{C}$, $M_{liq} = \text{batch}$) on limit apparent viscosity for a shear rate of 1000 s^{-1} of the products: raw Juice
950 (Lot A), enzyme treated juices with Ultrazym (Juice-Ult) and Pectinex (Juice-Pec), retentates of
951 microfiltration without enzyme (Juice CMF), with enzyme treatments (Juice-Ult CMF and Juice-Pec
952 CMF). Values with the same letters were not significantly different at $p < 0.05$.

953 **Figure 4.** Effect of transmembrane pressure (T_{mP}) on permeate flux (J_p) during crossflow
954 microfiltration of the juice ($T_{CMF} = 30^{\circ}\text{C}$, $U = 5 \text{ m}\cdot\text{s}^{-1}$, $MRR = 1$) after enzymatic treatment (Pectinex 300
955 $\mu\text{L}\cdot\text{kg}^{-1}$, $t_{liq} = 90 \text{ min}$, $T_{liq} = 30^{\circ}\text{C}$, $M_{liq} = \text{batch}$) using the four chosen membranes (Lot A).

956 **Figure 5.** Carotenoid content and bioaccessibility of the eight concentrates (Lot B) obtained according
957 to the combination of different parameters. C# is the concentrate corresponding to the essay #
958 according to the Plackett-Burman design (Mean and standard deviation from 3 repetitions).

959 **Figure 6.** Relative effect of operating parameters on carotenoid bioaccessibility (BC: β -carotene, BCX:
960 β -cryptoxanthin, LYC: lycopene) of concentrates (Lot B). Dose: enzyme dose, Mliq: liquefaction mode,
961 Tliq: liquefaction temperature, TCMF: crossflow microfiltration temperature, U: crossflow velocity,
962 Diaf: diafiltration, Past: pasteurization.

963 **Figure 7.** Relative effects of operating parameters on particle size distribution $D[4,3]$ and viscosity of
964 concentrates (Lot B). Dose: enzyme dose, Mliq: liquefaction mode, Tliq: liquefaction temperature,
965 TCMF: crossflow microfiltration temperature, U: crossflow velocity, Diaf: diafiltration, Past:
966 pasteurization.

967 **Supplementary files**

968 **Table S1.** pH, TA, TSS, SIS, TDM, turbidity in the juice (Lot A), Juice CMF the retentate of
969 microfiltration ($T_{CMF} = 30^{\circ}\text{C}$, $U = 5 \text{ m}\cdot\text{s}^{-1}$, $T_{mP} = 2.6 \text{ bar}$, obtained at $\text{MRR} = 1$ with the 4 membranes
970 mounted in series), Juice-Ult and Juice-Pec the enzyme treated juices with Ultrazym and Pectinex
971 ($300 \mu\text{L}\cdot\text{kg}^{-1}$, $t_{liq} = 90 \text{ min}$, $T_{liq} = 30^{\circ}\text{C}$, $M_{liq} = \text{batch}$), Juice-Ult and Juice-Pec the enzyme treated juices
972 with Ultrazym and Pectinex microfiltered

973 **Figure S1.** Particle size distribution in the Juice (Lot A), Juice CMF the retentate of microfiltration
974 ($T_{CMF} = 30^{\circ}\text{C}$, $U = 5 \text{ m}\cdot\text{s}^{-1}$, $T_{mP} = 2.6 \text{ bar}$, obtained at $\text{MRR} = 1$ with the 4 membranes mounted in
975 series), Juice-Ult and Juice-Pec the enzyme treated juices with Ultrazym and Pectinex ($300 \mu\text{L}\cdot\text{kg}^{-1}$, t_{liq}
976 = 90 min , $T_{liq} = 30^{\circ}\text{C}$, $M_{liq} = \text{batch}$).

977 **Figure S2.** Evolution of permeate flux according the MRR for three concentrates as examples C4, C5
978 and C8.

979

980

981

982

983

984

985

986

987

988

989

990

991

992

993

994

995

996

997

998

999

1000

1001

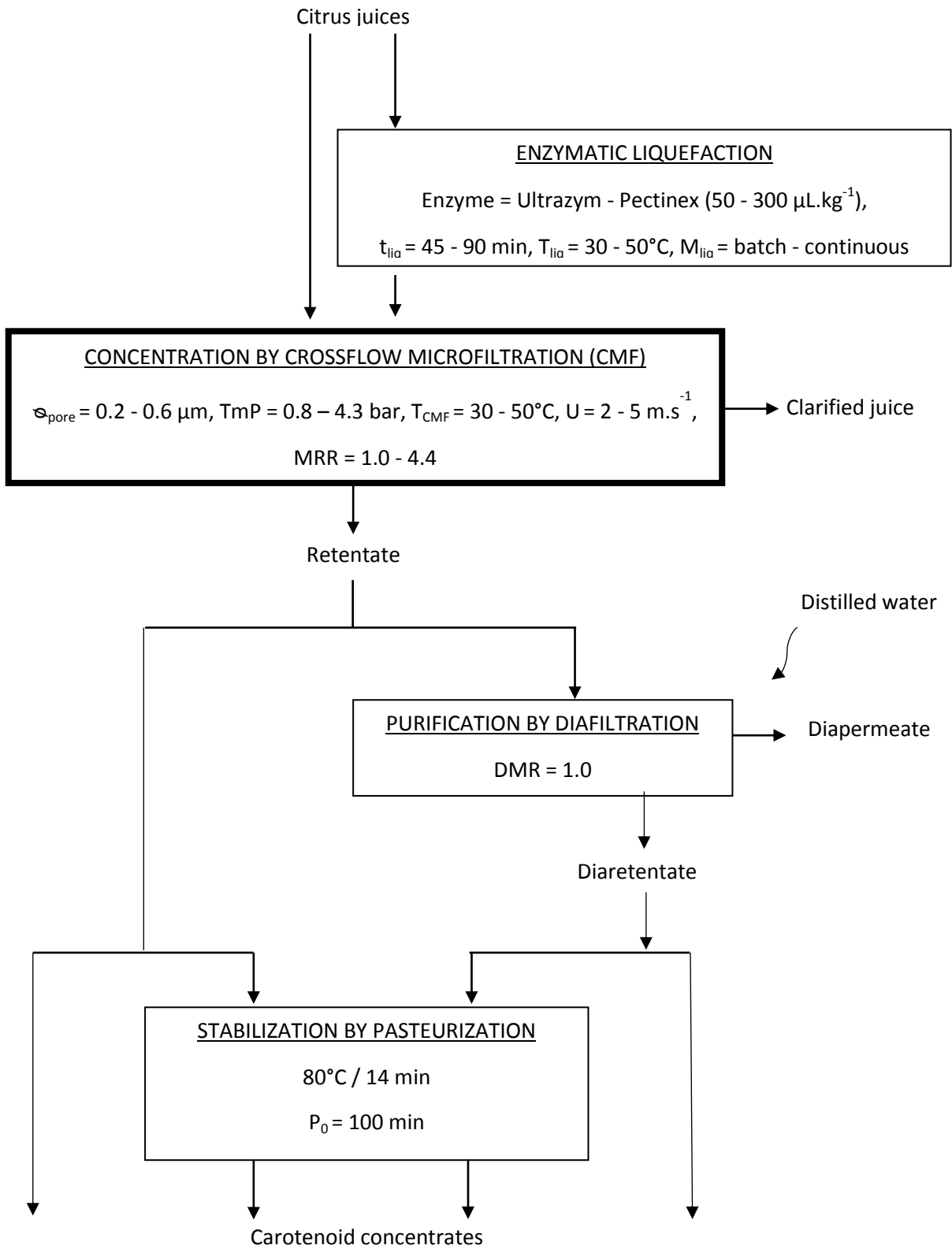
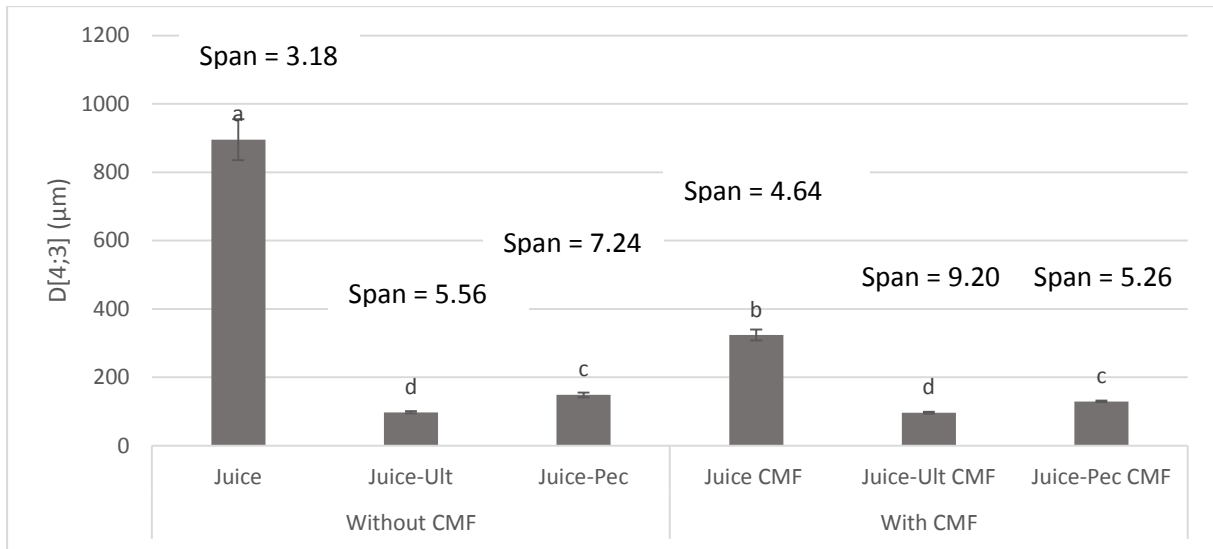


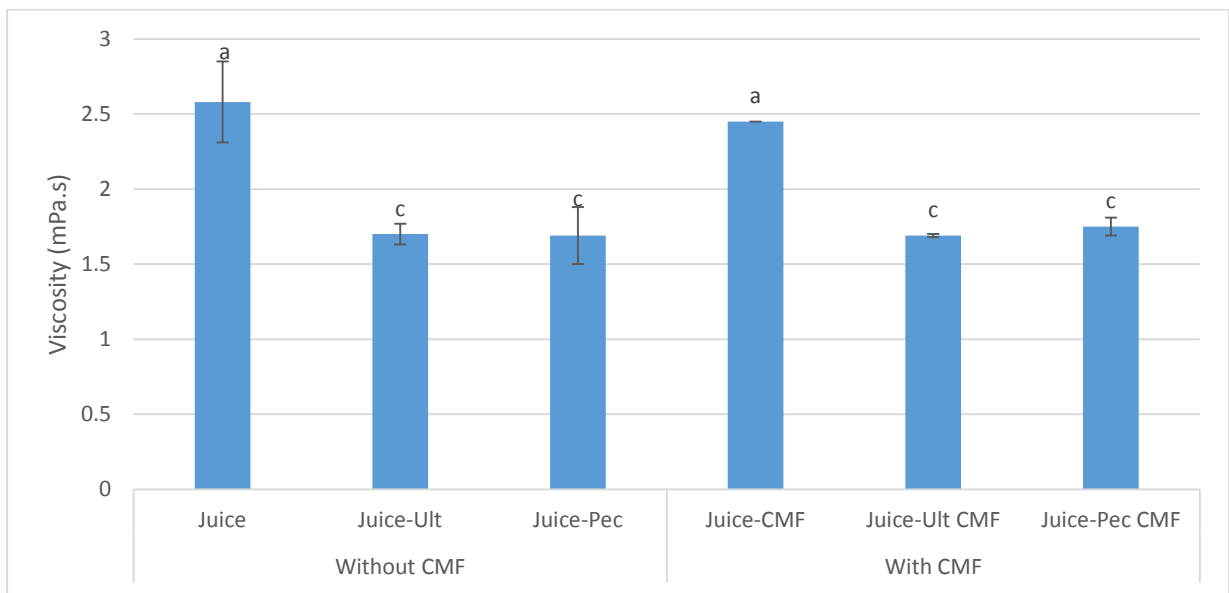
Figure 1. Process flow diagram of the experimental setup (see abbreviation list for meaning).



1002

1003 **Figure 2.** Effect of crossflow microfiltration ($T_{CMF} = 30^{\circ}C$, $U = 5 m.s^{-1}$, $TmP = 2.6 bar$, obtained at $MRR =$
 1004 1 with the 4 membranes mounted in series) and enzymatic treatment ($300 \mu L.kg^{-1}$, $t_{liq} = 90 min$, $T_{liq} =$
 1005 $30^{\circ}C$, $M_{liq} = batch$) on the mean volume diameter $D[4,3]$ and span of particles in the products: raw
 1006 Juice (Lot A), enzyme treated juices with Ultrazym (Juice-Ult) and Pectinex (Juice-Pec), retentates of
 1007 microfiltration without enzyme (Juice CMF), with enzyme treatments (Juice-Ult CMF and Juice-Pec
 1008 CMF). Values with the same letters were not significantly different at $p < 0.05$.

1009



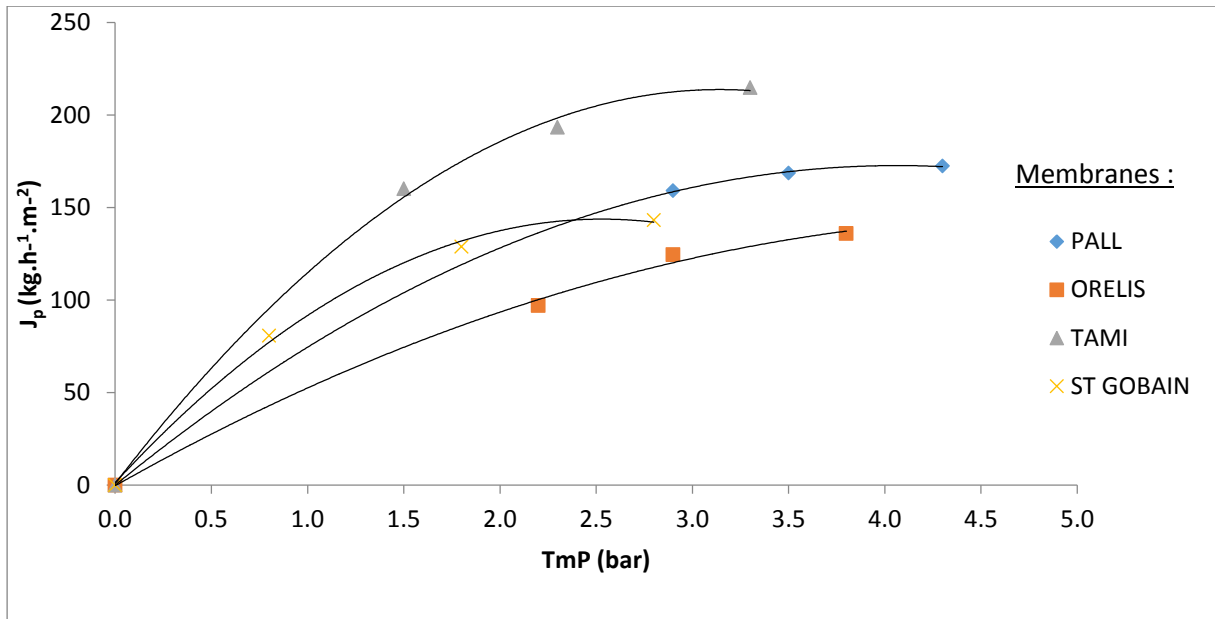
1010

1011 **Figure 3.** Effect of crossflow microfiltration ($T_{CMF} = 30^{\circ}C$, $U = 5 m.s^{-1}$, $TmP = 2.6 bar$, obtained at $MRR =$
 1012 1 with the 4 membranes mounted in series) and enzymatic treatment ($300 \mu L.kg^{-1}$, $t_{liq} = 90 min$, $T_{liq} =$
 1013 $30^{\circ}C$, $M_{liq} = batch$) on limit apparent viscosity for a shear rate of $1000 s^{-1}$ of the products: raw Juice
 1014 (Lot A), enzyme treated juices with Ultrazym (Juice-Ult) and Pectinex (Juice-Pec), retentates of
 1015 microfiltration without enzyme (Juice CMF), with enzyme treatments (Juice-Ult CMF and Juice-Pec
 1016 CMF). Values with the same letters were not significantly different at $p < 0.05$.

1017

1018

1019

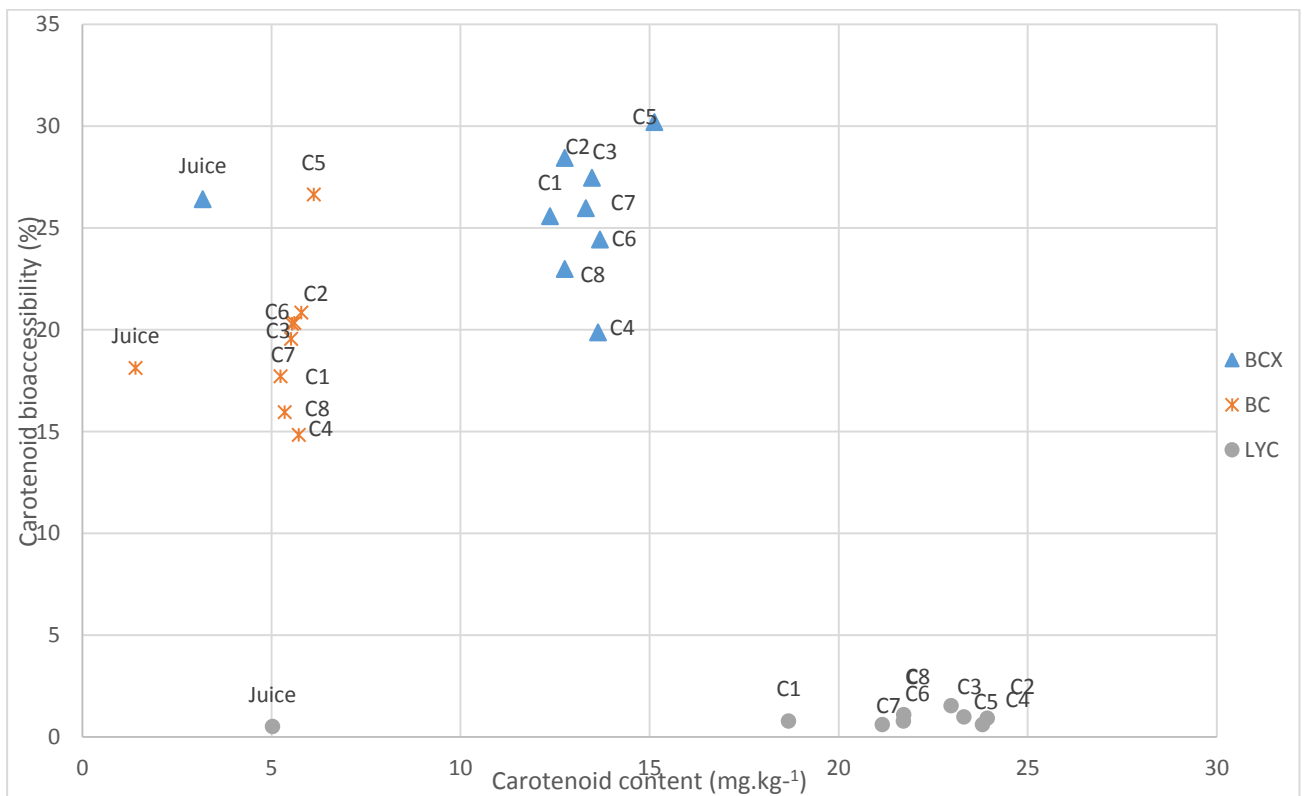


1020

1021 **Figure 4.** Effect of transmembrane pressure (TmP) on permeate flux (J_p) during crossflow
 1022 microfiltration of the juice ($T_{CMF} = 30^\circ\text{C}$, $U = 5 \text{ m}\cdot\text{s}^{-1}$, $MRR = 1$) after enzymatic treatment (Pectinex 300
 1023 $\mu\text{L}\cdot\text{kg}^{-1}$, $t_{liq} = 90 \text{ min}$, $T_{liq} = 30^\circ\text{C}$, $M_{liq} = \text{batch}$) using the four chosen membranes (Lot A).

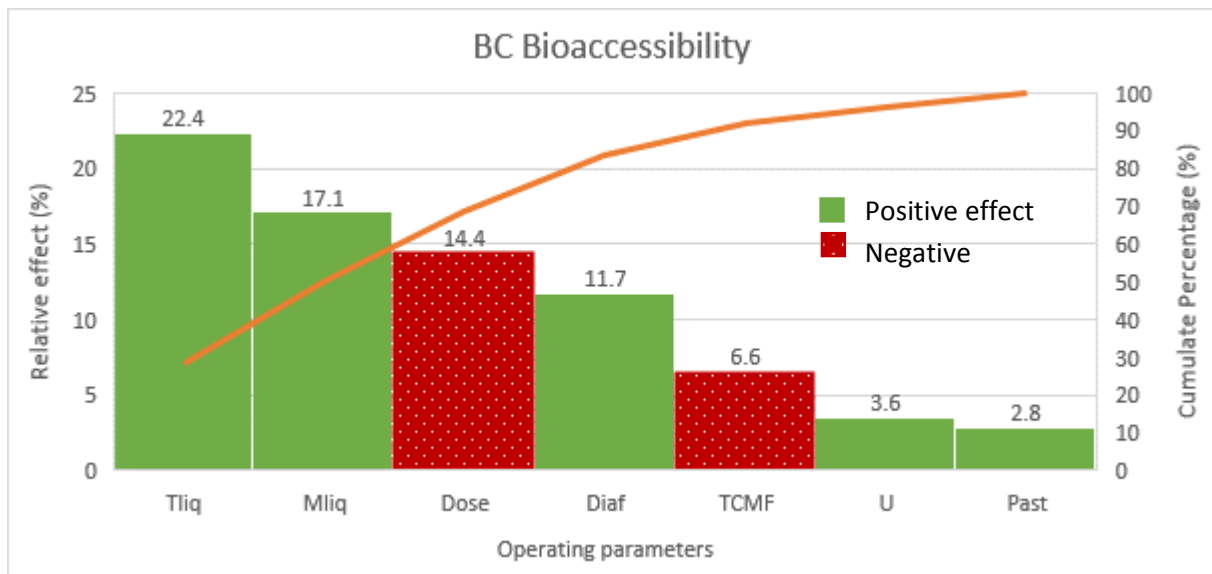
1024

1025

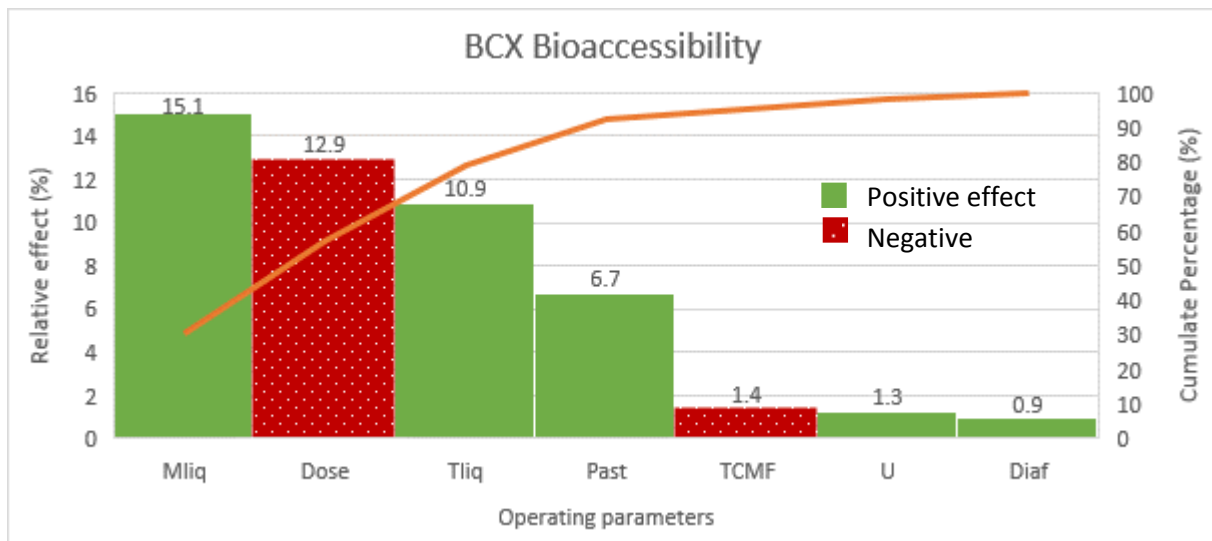


1026

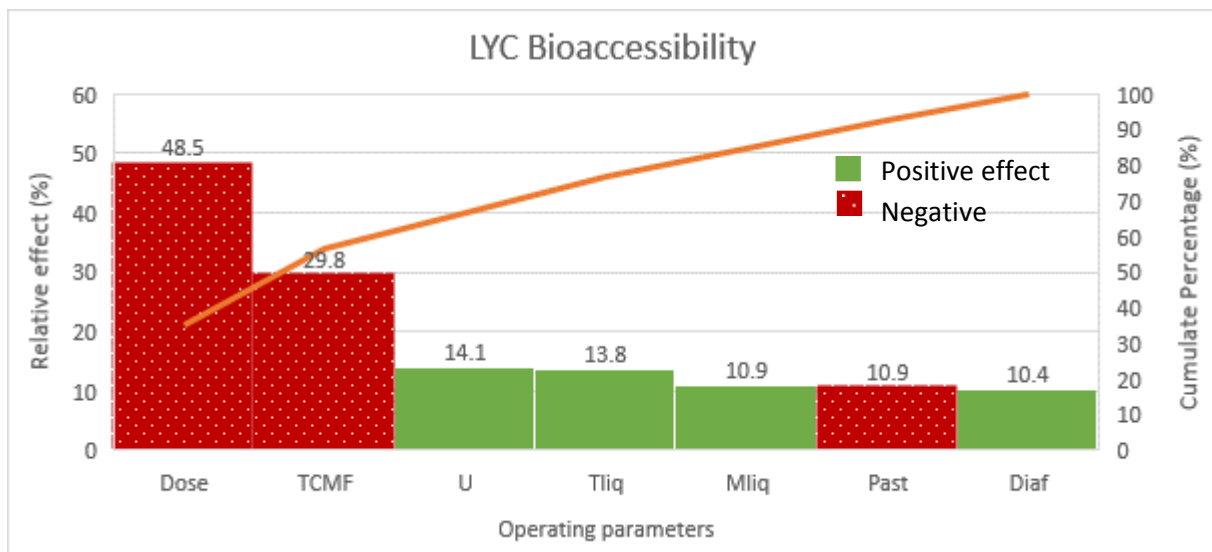
1027 **Figure 5.** Carotenoid content and bioaccessibility of the eight concentrates (Lot B) obtained according
 1028 to the combination of different parameters. C# is the concentrate corresponding to the essay #
 1029 according to the Plackett-Burman design.



1030



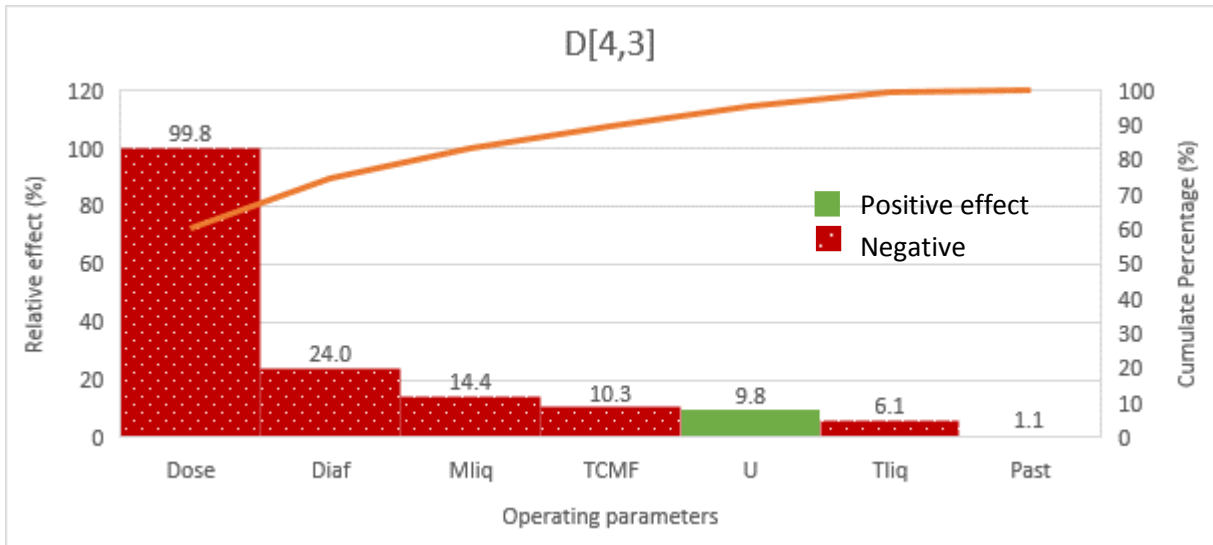
1031



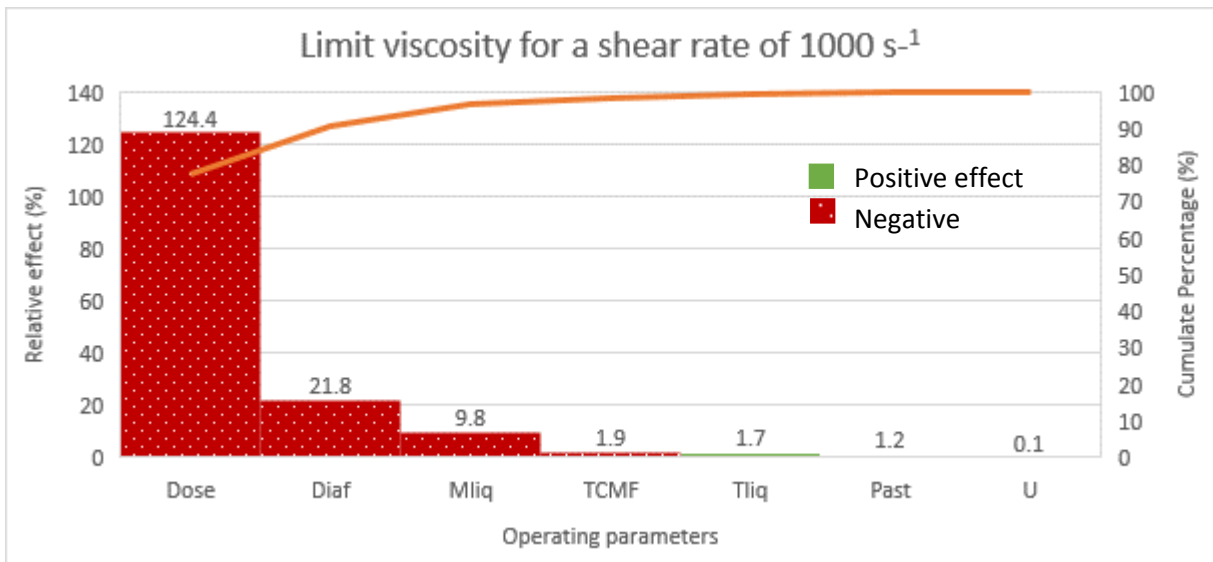
1032

1033 **Figure 6.** Relative effect of operating parameters on carotenoid bioaccessibility (BC: β -carotene, BCX: β -cryptoxanthin, LYC: lycopene) of concentrates (Lot B). Dose: enzyme dose, Mliq: liquefaction mode,
 1034 Tliq: liquefaction temperature, TCMF: crossflow microfiltration temperature, U: crossflow velocity,
 1035 Diaf: diafiltration, Past: pasteurization.
 1036

1037



1038



1039

1040 **Figure 7.** Relative effects of operating parameters on particle size distribution D[4,3] and viscosity of
 1041 concentrates (Lot B). Dose: enzyme dose, Mliq: liquefaction mode, Tliq: liquefaction temperature,
 1042 TCMF: crossflow microfiltration temperature, U: crossflow velocity, Diaf: diafiltration, Past:
 1043 pasteurization.

1044

1045

1046

1047

1048

1049

1050

1051

1052

1053

1054 **Table 1.** Main characteristics of the 4 tubular membranes chosen for crossflow microfiltration

Manufacturer	Pall-Exekia (Bazet, France)	Orelis (Salindres, France)	Tami Industries (Nyons, France)	Saint-Gobain (Cavaillon, France)
Material of active layer	Alumina (Al ₂ O ₃)	Zirconia (ZrO ₂)	Titanium oxide (TiO ₂)	Silicon carbide (SiC)
Average pore size (μm)	0.2	0.2	0.2	0.6
Internal diameter (mm)	7	7	7	6
Filtration area (cm ²)	55	55	55	43
Length (m)	0.25	0.25	0.25	0.25
Pristine membrane water permeability (kg.h ⁻¹ .m ⁻² .bar ⁻¹) ¹	1500 -1800	≈ 2000	2500 - 3500	≈ 5000
Average stabilized water permeability (kg.h ⁻¹ .m ⁻² .bar ⁻¹) ²	374 (102)	304 (62)	484 (132)	950 (257)

1055 ¹ from the suppliers, at 25 °C.1056 ² mean and standard deviation measured after at least 6 cleaning cycles, with tap water at 30°C, at
1057 TmP ranging from 2.5 bar to 3.4 bar and at U = 5 m.s⁻¹. Values used to verify cleaning efficiency after
1058 each trial.

1059

Table 2. Plackett-Burman experimental design used to identify the most influent operating parameters (Tami membrane, TmP = 2.6 bar, Ultrazym used as enzyme)

	Concentrates	C1	C2	C3	C4	C5	C6	C7	C8
Operating parameters	Enzyme dose ($\mu\text{L.kg}^{-1}$)	300	0	0	300	0	300	300	0
	Liquefaction Mode M_{liq}	Batch	Batch	Continuous	Continuous	Batch	Continuous	Batch	Continuous
	Liquefaction temperature T_{liq} ($^{\circ}\text{C}$)	30	30	50	30	50	50	50	30
	Filtration temperature T_{CMF} ($^{\circ}\text{C}$)	30	50	50	50	30	30	50	30
	Crossflow velocity U (m.s^{-1})	5	2	5	5	5	2	2	2
	Diafiltration	No	Yes	No	Yes	Yes	Yes	No	No
	Pasteurization	Yes	Yes	Yes	No	No	Yes	No	No

1063 **Table 3.** Physico-chemical, structural characteristics and carotenoid content and bioaccessibility of
 1064 initial citrus juice (mean and standard deviation from n = 3).

		Lot A	Lot B	Lot C
pH		3.51 (0.15)	3.45 (0.02)	3.49 (0.08)
TA (g.kg ⁻¹)		8.6 (0.2)	10.4 (0.5)	10.8 (0.6)
TSS (g.kg ⁻¹)		99.8 (1.6)	108.0 (0.1)	111.3 (1.1)
SIS (g.kg ⁻¹)		3.2 (0.2)	3.1 (0.2)	3.1 (0.3)
TDM (g.kg ⁻¹)		100.9 (2.0)	110.9 (1.0)	105.0 (0.1)
Limit viscosity (1000 s ⁻¹) (mPa.s)		2.43 (0.13)	3.24 (0.24)	2.96 (0.09)
D[4,3] (µm)		896 (60)	912 (17)	922 (21)
Span		3.18 (0.53)	3.12 (0.47)	3.16 (0.27)
Turbidity (NTU)		2169 (147)	3840 (165)	ND
Carotenoid Content (mg.kg ⁻¹)	BC	ND	1.41 (0.04)	1.17 (0.03)
	BCX	ND	3.19 (0.35)	2.52 (0.02)
	LYC	ND	5.03 (0.16)	6.07 (0.10)
Carotenoid Bioaccessibility β (%)	BC	ND	18.12 (0.51)	12.92 (0.43)
	BCX	ND	26.41 (0.50)	22.70 (0.71)
	LYC	ND	0.51 (0.02)	0.75 (0.13)
RAE (µg/ 250g of juice)		ND	62.6 (4.5)	50.6 (0.8)
RAE* (µg/ 250g of juice)		ND	14.1 (1.4)	9.1 (0.4)
RDA (%)		ND	7.8 (0.6)	6.3 (0.1)

*Not determined.

1065

1066

1067

1068 **Table 4.** Effect of enzymatic treatment ($300 \mu\text{L.kg}^{-1}$, $t_{\text{liq}} = 90 \text{ min}$, $T_{\text{liq}} = 30^\circ\text{C}$, $M_{\text{liq}} = \text{batch}$) on the
1069 stabilized permeate flux J_p during the microfiltration ($T_{\text{CMF}} = 30^\circ\text{C}$, $\text{MRR} = 1$) of citrus juice (Lot A) for
1070 different membrane / transmembrane pressure combinations.

J_p ($\text{kg.h}^{-1}.\text{m}^{-2}$)	PALL (3.5 bar)	ORELIS (2.9 bar)	TAMI (2.3 bar)	SAINT-GOBAIN (1.8 bar)
Raw juice	109.7	105.8	155.2	122.7
Treated with Ultrazym	165.7	113.6	185.8	130.2
Treated with Pectinex	168.7	124.5	193.3	128.8

1071

1072

1073

1074 **Table 5.** Average permeate flux (J_p), physico-chemical and structural characteristics and carotenoid
 1075 analysis of the 8 concentrates obtained according to the combination of different parameters (lot B).
 1076 C# is the concentrate corresponding to the Plackett-Burman design (Table 2) using the Tami
 1077 membrane, TmP = 2.6 bar and Ultrazym as enzyme (Mean and standard deviation from 3).

		C1	C2	C3	C4	C5	C6	C7	C8
J_p ($3 < \text{MRR} < 4.4$) ($\text{kg}\cdot\text{h}^{-1}\cdot\text{m}^{-2}$)		76.1	28.1	55.6	120.8	38.3	48.2	92.1	15.3
Flux instability $\partial J_p / \partial \text{MRR}$ ($3 < \text{FRM} < 4.4$) ($\text{kg}\cdot\text{h}^{-1}\cdot\text{m}^{-2}$)		1.6	2.4	9.6	4.5	8.0	7.6	5.6	0.2
TSS ($\text{g}\cdot\text{kg}^{-1}$)		126.0 ^a (2.6)	51.7 ^b (0.6)	119.3 ^c (0.6)	49.3 ^b (1.2)	51.3 ^b (1.5)	59.7 ^d (0.6)	125.0 ^a (1)	122.0 ^e (2)
SIS ($\text{g}\cdot\text{kg}^{-1}$)		12.2 ^{ef} (0.1)	14.7 ^a (0.4)	13.7 ^b (0.5)	12.9 ^{cd} (0.1)	13.1 ^c (0.2)	12.8 ^{cd} (0.0)	12.0 ^f (0.5)	12.6 ^{de} (0.2)
TDM ($\text{g}\cdot\text{kg}^{-1}$)		115.4 ^{bc} (0.6)	62.1 ^d (0.4)	117.3 ^b (2.2)	51.4 ^f (1.4)	60.0 ^d (1.7)	53.9 ^e (1.0)	114.9 ^c (1.0)	120.6 ^a (1.0)
Limit viscosity (1000 s^{-1}) (mPa.s)		3.66 ^a (0.03)	11.93 ^b (0.21)	14.67 ^c (0.06)	2.42 ^d (0.05)	12.13 ^e (0.15)	2.81 ^d (0.08)	3.54 ^f (0.03)	14.57 ^c (0.25)
D[4,3] (μm)		98 ^a (4)	178 ^b (6)	238 ^c (21)	68 ^d (2)	196 ^e (10)	62 ^d (1)	59 ^d (4)	246 ^c (26)
Span		6.22 (0.58)	3.91 (0.24)	4.18 (0.59)	8.54 (0.65)	2.24 (0.10)	10.98 (0.28)	5.76 (0.65)	4.48 (0.56)
Turbidity (NTU)		16367 ^a (90)	19110 ^b (385)	15570 ^c (576)	13730 ^d (337)	15850 ^{ac} (311)	14280 ^d (171)	16020 ^{ac} (259)	16993 ^{ae} (200)
Carotenoid Content ($\text{mg}\cdot\text{kg}^{-1}$)	BC	5.24 ^a (0.13)	5.79 ^{ab} (0.12)	5.55 ^{ab} (0.73)	5.73 ^{ab} (0.51)	6.12 ^b (0.09)	5.61 ^{ab} (0.21)	5.52 ^a (0.11)	5.35 ^b (0.15)
	BCX	12.37 ^c (0.04)	12.76 ^{bc} (1.19)	13.48 ^{bc} (1.21)	13.64 ^b (1.14)	15.13 ^a (0.67)	13.69 ^b (0.40)	13.32 ^{bc} (0.26)	12.76 ^{bc} (1.19)
	LYC	18.68 ^d (0.37)	23.94 ^a (1.47)	23.32 ^{abc} (2.39)	23.81 ^{ab} (0.74)	22.98 ^{abc} (0.93)	21.72 ^{bc} (1.26)	21.16 ^c (0.45)	21.73 ^{bc} (1.16)
Carotenoid Bioaccessibility β_i (%)	BC	17.71 ^{cd} (2.10)	20.84 ^b (3.05)	20.28 ^{bc} (3.62)	14.83 ^d (1.85)	26.64 ^a (1.93)	20.33 ^{bc} (4.00)	19.55 ^{bcd} (1.88)	15.95 ^{cd} (2.46)
	BCX	25.57 ^{bc} (1.76)	28.43 ^b (1.88)	27.46 ^b (2.36)	19.87 ^d (2.38)	30.20 ^a (0.39)	24.42 ^{bc} (2.46)	25.96 ^b (2.46)	22.97 ^{cd} (2.66)
	LYC	0.78 ^c (0.07)	0.91 ^b (0.12)	0.97 ^b (0.14)	0.60 ^c (0.17)	1.53 ^a (0.01)	0.77 ^c (0.14)	0.60 ^c (0.05)	1.09 ^b (0.17)
RAE ($\mu\text{g}/250\text{g}$ of concentrate)		238.0 (3.1)	253.5 (14.9)	256.0 (27.8)	261.5 (22.5)	285.1 (25.7)	259.5 (8.5)	253.8 (5.0)	244.4 (15.5)
RAE* ($\mu\text{g}/250\text{g}$ of concentrate)		52.3 (5.2)	62.9 (10.2)	62.0 (14.1)	45.9 (9.5)	81.5 (10.2)	58.6 (10.1)	58.5 (6.7)	48.3 (9.6)
RDA (%)		29.8 (0.4)	31.7 (1.9)	32.0 (3.5)	32.7 (2.8)	35.6 (3.2)	32.4 (1.1)	31.7 (0.6)	30.6 (1.9)
RDA* (%)		6.5 (0.7)	7.9 (1.3)	7.8 (1.8)	5.7 (1.2)	10.2 (1.3)	7.3 (1.3)	7.3 (0.8)	6.0 (1.2)

1078 **Table 6.** Impact of a low enzyme dose on average permeate flux (J_p) and characteristics of
 1079 concentrates obtained in the most favorable conditions for carotenoid bioaccessibility (enzyme
 1080 liquefaction in batch mode at 50°C, $T_{CMF} = 30^\circ\text{C}$, $U = 5.\text{m}.\text{s}^{-1}$, with diafiltration and no pasteurization)
 1081 (Lot C) (Mean and standard deviation from 3 repetitions).

		Concentrate without enzyme (reference)	Concentrate after Ultrazym liquefaction at 50 $\mu\text{L}.\text{kg}^{-1}$
J_p (3 < FRM < 4.4) ($\text{kg}.\text{h}^{-1}.\text{m}^{-2}$)		40.5	81.4
Flux instability $\partial J_p / \partial \text{MRR}$ (3 < FRM < 4.4) ($\text{kg}.\text{h}^{-1}.\text{m}^{-2}$)		6.2	1.2
TSS ($\text{g}.\text{kg}^{-1}$)		50.3 ^a (0.6)	53.3 ^b (0.6)
SIS ($\text{g}.\text{kg}^{-1}$)		10.9 ^a (0.1)	10.7 ^a (0.3)
TDM ($\text{g}.\text{kg}^{-1}$)		57.5 ^a (0.1)	58.3 ^b (0.1)
Limit viscosity (1000 s^{-1}) ($\text{mPa}.\text{s}$)		9.26 ^a (0.08)	2.64 ^b (0.08)
D[4,3] (μm)		233 ^a (17)	230 ^a (11)
Span		3.41 (0.43)	3.51 (0.32)
Carotenoid Content ($\text{mg}.\text{kg}^{-1}$)	BC	3.87 ^a (0.11)	4.00 ^a (0.21)
	BCX	9.07 ^a (0.13)	8.96 ^a (0.37)
	LYC	20.41 ^a (0.83)	21.78 ^a (1.00)
Carotenoid Bioaccessibility β (%)	BC	15.79 ^a (1.47)	16.60 ^a (0.45)
	BCX	27.02 ^a (3.18)	29.43 ^a (2.26)
	LYC	0.94 ^a (0.13)	0.89 ^a (0.05)
RAE ($\mu\text{g}/250\text{g}$ of concentrate)		175.1 (3.7)	176.7 (8.2)
RAE* ($\mu\text{g}/250\text{g}$ of concentrate)		38.3 (4.9)	41.3 (4.3)
RDA (%)		21.9	22.1
RDA* (%)		4.8	5.2